Aalto University
School of Science
Degree Programme in Computer Science and Engineering

Mudassar Abbas

Statistical Estimation of Wild Animal Population in Finland:

A Multiple Target Tracking Approach

Master's Thesis
Espoo, December 9, 2011

Supervisor:	Professor Jouko Lampinen
Instructors:	Docent Simo Särkkä Docent Aki Vehtari

Aalto University
School of Science
Degree Programme in Computer Science and Engineering

ABSTRACT OF
MASTER'S THESIS

Author:	Mudassar Abbas		
Title:	Statistical Estimation of Wild Animal Population in Finland: A Multiple Target Tracking Approach		
Date:	December 9, 2011	**Pages:**	68
Professorship:	Computational Engineering	**Code:**	S-114
Supervisor:	Professor Jouko Lampinen		
Instructors:	Docent Simo Särkkä Docent Aki Vehtari		

Control and management of wild animals, especially large carnivores, is an important task for game and wildlife management authorities all over the world. Central to the scheme of wild animal conservation is the population size estimation methodology which depends on the used data sampling technique. The index based data sampling method has been found suitable in the case of large carnivores. On the other hand, telemetry data has been used to learn the individual movement of animals. Subsequently, mathematical modeling is utilized in order to learn both animal population dynamics and animal movement behavior. In that context, stochastic state-space models have proved to be appropriate for handling uncertainty that occurs in the process and observation models.

This thesis provides a novel approach for the estimation of wild animal population. We utilize the state-space modeling framework as well as animal movement models on an unconventional observation and index based dataset. We formulate the problem as a conditionally linear Gaussian state-space model and recursively estimate the state of the animals. More specifically, we reformulate the problem as a special case of multiple target tracking, which can be solved by using Bayesian optimal filtering methodology. The solution to the problem of tracking an unknown number of targets is exactly applicable to our animal observation datasets.

Keywords: Bayesian Inference, Sequential Monte Carlo Method, Kalman Filter, Multiple Target Tracking, Data Association

Language: English

Acknowledgements

I would like to express my sincere gratitude to Dr. Simo Särkkä for his immense support and guidance throughout the development of this project and thesis. I also wish to extend my deepest appreciation to Dr. Aki Vehtari for his continuous advice and encouragement. My sincere appreciation is extended to Prof. Jouko Lampinen for his support.

I would also like to extend my sincere appreciation to Mr. Samuli Heikkinen and Mr. Mika Kurkilahti from the Finnish Game and Fisheries Research Institute for their contributions to the project.

Special thanks to Mr. Ville Väänänen for his insightful feedback on the thesis and contributions to the project. I also wish to thank M.Sc. Marianne Hanhela for her contributions to the project. I am also thankful to all the colleagues at the Biomedical Engineering and Computational Science department for providing a special working environment. I wish to extend my appreciation to M.Sc. Jouni Hartikainen for his help and support.

I am immensely grateful to my parents for providing me the opportunities to follow my dreams. I am also especially grateful to all my friends and family for their love and support.

Espoo, December 9, 2011

Mudassar Abbas

Abbreviations and Acronyms

MCMC	Markov Chain Monte Carlo
SIS	Sequential Importance Sampling
SIR	Sequential Importance Resampling
SDE	Stochastic Differential Equation
CRW	Correlated Random Walk
O-U	Ornstein-Uhlenbeck
GPS	Global Positioning System
EKF	Extended Kalman Filter
UKF	Unscented Kalman Filter
RBPF	Rao-Blackwellized Particle Filter
MHT	Multiple Hypothesis Tracking
GNN	Global Nearest Neighbor
SNF	Strongest-neighbor Filter
PDAF	Probabilistic Data Association Filter
JPDA	Joint Probabilistic Data Association
RBMCDA	Rao-Blackwellized Monte Carlo Data Association
YKJ	Yhtenäiskoordinaatisto (Uniform Coordinate System)

Contents

List of Tables

List of Figures

Chapter 1

Introduction

For more than half a century now it has been appreciated that wild animals enact an essential role in maintaining the biological diversity of the ecosystem. Therefore, considerable effort has been taking place all over the world for the conservation of wild animals especially in the case where some species face extinction. However, at times a species can be given the 'pest' status when it exceeds a certain limit of abundance and it can cause considerable damage to human life and property (Delahay and Wilson, 2001). Then a reasonable balance would have to be insured with appropriate control programs. These are the fundamental reasons for the control and management of wild animal populations. Central to the scheme of wild animal population monitoring and management is the estimation of the population size. A large number of methods have been developed and deployed by biologists, ecologists and wildlife managers to attain this goal (Southwood and Henderson, 2000; Schwarz and Seber, 1999).

Methods used in estimating the size of wild animal population can be classified to two main groups: true abundance methods and index based methods (Delahay and Wilson, 2001). True abundance can further produce two types of count: a complete count (census) and an incomplete count (survey). A complete count can be obtained when the assumption that all the animals would be counted is true while an incomplete count only samples from a proportion of the total animal population. Surveys can be conducted by using vehicles, airplanes and imagery technologies. A more favored statistical approach of surveying is the capture-recapture method which is mainly used in fisheries. This approach implies that the species is in some way caught and marked by the field researchers. The methods of marking include tagging, banding and painting. This method of sample collection is also known as mark-recapture in animal ecology.

On the other hand an index based methodology requires that the field personnel avoid direct interaction with the animal. In this case observation of field-signs (remains) of the animals is a crucial methodology, for example, observation of habitat structure and carcasses of dead prey, identifying tracks (foot-prints) and marks left on plants, and finding feces and animal hair. More recent advances in index based techniques consist of methods like DNA analysis of hair, feather, feces, dung, saliva and shed skin (Mills et al., 2000). Moreover, DNA analysis can also be used in capture-recapture where the sample is taken directly from the body of the animal (Madon et al., 2011). However, capture-recapture methods involve significant human effort and expenditure especially in the case of large carnivores because of their secretive and nocturnal nature. At the same time predicting the exact home range of large carnivores is very difficult. Therefore, incomplete counts and index based approaches appear more practical and often preferred especially by wild life managers for monitoring of large areas (Witmer, 2005; Pollock et al., 2002).

More often, surveys can be conducted sequentially year after year to learn the dynamics of animal population. Consequently, prediction and management decisions have to be based on dynamic population models. These models can be formulated as population-growth models which consist of parameters indicating population-growth rate. A population can grow because of birth and immigration but simultaneously reduce due to death and emigration. Similarly, dynamic population models can be based on an age-structure formulation. The age-structure based models divide the total animals surveyed into age groups. In these models parameters like survival and reproduction rate replace the birth and death count parameters. Furthermore, population models can be density dependent or density independent with the former being more complex kind of models.

Realistic population dynamics models must incorporate the stochasticity inherent in the actual underlying processes. Process variation and the variation due to sampling necessitates statistical approaches that incorporate these uncertainties into the models. Therefore, a statistical modeling approach known as state-space modeling has been widely acknowledged as a flexible and appropriate approach to population dynamics models (Buckland et al., 2004b, 2007). Although population dynamic models can include animal movement (immigration, emigration) in the form of probability distributions (probability of moving from one location to the other), more dense positional data available with the advancement in radio telemetry and GPS telemetry has allowed scientists to study animal movement and habitat behavior on an individual scale (Börger et al., 2008). The classical models of individual animal movement comprises of stochastic differential equations (SDE) (Brillinger et al., 2002; Preisler et al., 2004). Since observational data from telemetric devices is also prone to error (noise), use of statistical approaches, specifically state-space modeling, has been favored in order to link the dynamic models of animal movement to the observational data (Patterson et al., 2008).

Modeling of individual animal movement based on telemetry data has increased the knowledge about many social and habitual behaviors of species. However, it has been less beneficial for the management and conservation of animals on a large scale (Morales et al., 2010). This is mainly due to the high expenses of acquiring telemetry data and low feasibility of tagging a large number of animals. Therefore, methods of estimating animal populations based on surveys and index data have to be developed and improved with a focus on utilizing the current computational power of modern computers. In this thesis, we propose a novel approach based on an unconventional observation and index based survey data. We utilize both state-space modeling framework and animal movement models in order to estimate the animal population.

1.1 Overview of Problem

We focus on the analysis of sampling data, which is based on both field-signs and direct sightings of the animals. A single record in the dataset can consist of information about a single individual or group of animals (family or pack). The information can be either from direct sightings or field-signs of the animals. Field signs consist of foot print measurements, feces observation, carcass of dead animal or prey and in some cases habitat structure or animal marks. The data collection process is based on observations obtained on a regular basis throughout the year from almost every part of Finland. The accumulated datasets consist of a far greater number of observations than the actual number of animals. On the contrary, in the index-data based population estimation methods, the population survey is usually conducted in smaller regions and shorter time frames and the result of estimation is extrapolated to larger regions.

The data collection method in our case is unconventional and the standard methodology of animal abundance estimation becomes inapplicable. The present method used to estimate population size from this data requires a significant amount of manual work which involves sorting the information and finding duplicate observations of the same individual or group of animals that have been observed by multiple observers. Therefore, we propose a state of the art technique which solves the current problem of population estimation from the unusual data source computationally, without the need for manual work. We formulate the problem as a conditionally linear Gaussian state-space model and recursively estimate the state of the animals. More specifically, from the engineering perspective this strategy is known as optimal filtering.

The problem of estimating the state of multiple targets from noisy measurements generated by multiple sources is referred to as multiple target tracking and data association problem. This is an application area of optimal filtering. Furthermore, the methodology of data association for an unknown number of targets is exactly applicable to our animal observation datasets. In this thesis, we demonstrate the applicability of *Rao-Blackwellized Monte Carlo data association* (RBMCDA) (Särkkä et al., 2007) algorithm which solves the problem of multiple target tracking and data association in the case of 'an unknown number of targets'.

1.2 Structure of Thesis

The organization of this thesis is as follows: the general methods of estimating population size and the background of multiple target tracking methodology is covered with detail in Chapter 2, Chapter 3 presents the materials, methods and models utilized in the thesis, Chapter 4 shows the results of the study, and Chapter 5 presents the conclusion and discussions.

Chapter 2

Background

2.1 Finnish Politics and Animal Conservation

Concern has prevailed regarding the extinction of some very rare wild animals among naturalists, scientists, politicians and common people of Finland for the past fifty years. Nature reserves and wilderness areas of Finland have been home to four large carnivores; brown bear (Ursus arctos), wolf (Canis lupus), wolverine (Gulo gulo) and lynx (Lynx lynx). Since the beginning of the twentieth century the populations of all four of these fascinating animals has been in decline.

Brown Bear (Ursus arctos)

The brown bear is the national animal of Finland. The estimate of bear population before the hunting season in 2009 was 1850 to 1950 and at the end of 2009 was 1150 to 1200 (Wikman, 2010). The population density is higher in eastern Finland close to the Russian border. The brown bear was nearly extinct in Finland around the beginning of the twentieth century but population has steadily increased since 1970 (Katajisto, 2006), mainly due to migration of bears from Russia.

Wolf (Canis lupus)

Wolf is the most controversial large carnivore in Finland since it causes the highest threat to livestock, reindeer husbandry and humans. It is for this reason that it has the smallest population size among the large carnivores of Finland. The estimate of wolf population in Finland at the end of 2009 was 150 to 160 (Wikman, 2010). The population density is higher in the eastern regions. Wolves became extinct in the early twentieth century due to major hunting expeditions. Wolves have also been subject to severe illegal poaching activities.

Lynx (Lynx lynx)

Lynx has the highest population among the large carnivores of Finland with about 2200 to 2300 individuals reported at the end of 2009 (Wikman, 2010). People have a more benign attitude towards the lynx or wild cat although it is a very active predator (Liukkonen et al., 2009). Lynx has an even population density throughout Finland and the numbers have been increasing since it was protected.

Wolverine (Gulo gulo)

Wolverine is the most elusive animal among the large carnivores of Finland due to its less dense population structure and large dispersal ability. Population statistics claim that about 150 to 170 individuals were present at the end of 2009 (Wikman, 2010). It is also one of the most hunted and endangered animal populations of Finland. The wolverine was nearly extinct until it was protected in 1982.

Organization

The Ministry of Agriculture and Forestry is responsible for the population conservation of wild animals in Finland. Legislation concerning hunting licenses and management plans are approved by the ministry while these plans are based on research conducted by the Finnish Game and Fisheries Research Institute in particular. Other organizations which aid the research include, The Hunters Central Organization which provides sighting data and the Game Management district authorities. The Game Management district authorities license the hunting of animals under the supervision of the Ministry of Agriculture and Forestry based on the population statistics provided by the Finnish Game and Fisheries Research Institute.

The debate over large carnivore population management largely exists because of the threat posed by large carnivores to livestock and reindeer husbandry. While the wild life conservation legislations impose strict laws over the hunting of endangered species, the farmers and herders have valid reasons for employing safety measures against the threat caused by wild animals to their property and livestock. However, the large carnivore population in Finland has suffered not merely because of hunting and poaching but also due to other environmental and ecological changes in the natural habitat of the animals.

2.2 Animal Abundance

Methods for estimating animal abundance (How many are there?) depend on many factors: landscape of the area where the study or monitoring is taking place, type of specie which is being studied or monitored and the resources available to conduct the study or monitoring. Therefore, careful design of the estimation methods and procedures is of fundamental importance before initiating the actual field and analysis work (Witmer, 2005; Pollock et al., 2002).

2.2.1 Estimation Methods

Below, we briefly explain some of the well-known and standard approaches used in estimating animal abundance. These approaches apply to data obtained through specific sampling methods or surveys conducted in smaller regions in a fixed time frame. The individual count obtained through these surveys is often used to estimate the population density for a small region and the density is extrapolated for larger areas. However, we need to analyze our data in a more unconventional way because it is based on unrestricted random observations obtained from a very large area and over a longer time frame. Further details about the collection of data can be found in Chapter 3.

Strip and Quadrat Plots

This is a simple method based on counting the animals or field-signs, for example, feces or foot-prints, over a random set of plots known as sample units. Basically, the whole region or area, where the animal population estimation has to be accomplished, is divided in to smaller regions which can be square or rectangular in shape. The method of selecting the regions for sampling can vary, more specifications on sampling procedures can be found in (Anderson, 2001; Thompson et al., 1998). If random sampling is used and the animals can be directly observed then the method of estimation consists of the following steps:

- Dividing the whole region into a total of S number of sample units and choosing s number of sample units randomly where the census would be conducted.
- Counting the total number of animals n in each of the randomly chosen sample units s:

$$\bar{n} = \frac{1}{s} \sum_{i=1}^{s} n_i \ . \tag{2.1}$$

- The abundance estimate can be obtained by multiplying total sampling units S with $\bar{n}$ as

$$\hat{n} = S\ \bar{n}\ . \tag{2.2}$$

The abundance estimator can also be divided by the total area of the sampling units to calculate the population density estimate. Furthermore, a population indices estimate can also be obtained in case of observation of the field-signs. A single index must be a constant ratio for the whole population, that is, if the count of indices doubles then it can be proposed that the whole population has doubled (Schwarz and Seber, 1999).

Distance Sampling

This method mainly consists of two types; line transects and point counts. Line transects usually involves an observer moving by foot or in a vehicle along a random path and sighting the animals. The abundance is then calculated as number of animals sighted divided by the detection probability which is based on the distance between the observer and the animal. The detection probability also depends on the terrain detail, for example, it is higher for plain regions and lower for hilly areas. If an aerial survey is conducted using this method then the detection probability is not merely dependent on the distance between the animal and the observer but many other factors would be involved as well (Buckland et al., 2004a).

Capture-recapture

This method involves marking or tagging of animals during the initial sampling and then releasing them for the second sampling phase. The next sampling phase consists of marked and unmarked animals and estimation based on this data includes different methods and assumptions (Pollock, 2000; Buckland et al., 2000). One of the more well known methods to estimate the abundance with capture-recapture data is the Lincoln-Petersen model (Seber, 1986). This method comprises of a few assumptions; 1- only single recapture event, 2- closed population (excluding births, deaths or movement outside the region of study), 3- both recapture events have equal capture probabilities and 4- the marks or tags remain intact. If n_1 is the number of individuals captured and marked during the initial sampling, n_2 is the number of unmarked individuals during the second sampling and m_2 the number of recaptured individuals then the estimator is given by

$$\hat{n} = \frac{n_1\ n_2}{m_2}\ . \tag{2.3}$$

Removal Methods

Removal methods include two well-known models; the catch-effort model and the change-in-ratio model. Catch-effort models have primarily been used in fisheries with the assumptions that the population is closed and the probability of each individual being caught is equal. The catch per effort decreases with more individuals being caught (removed from the population) because there would be less individuals remaining to be caught. Change-in-ratio methods require the population to be closed and the population to be divided in to two groups, for example, male and female, adult and infant or two different species. The idea is to remove more individuals from one of the groups and observe the change-in-ratio during the resampling phase. Estimating the change-in-ratio before and after the sampling reveals other population parameters as well (Seber, 1986).

Index Scores

This method is used when only the field-signs of the animals can be observed. The assumption is that the frequency of observations is related to the actual number of animals. This method provides a relative estimate of abundance or “Index” of population density (Schwarz and Seber, 1999). Estimate of animal abundance can be deduced from “index scores” if they can be adjusted with estimates from another formal estimation method used in parallel (Delahay and Wilson, 2001).

2.2.2 Population Dynamics Modeling

Next, we shall briefly discuss some of the well-known population dynamics models. These models require sampling of specific parameters during the surveys, for example, birth date/time, death, movement in and out of sampling region and age-structure of the population. This information is obtained usually by capturing and tagging animals. However, this information is unavailable in our data because it is sighting and index based which restricts the use of these models. Nevertheless, the estimation method we have used can incorporate population dynamics models as well.

Detecting each animal with the same certainty is hardly possible, observations can be biased due to insufficient field related experience of the observer, tags and marks can be misplaced or lost, and most importantly surveys on a large geographical area and a longer time scale must be able to address an open population (births, deaths and movement) (Schwarz and Seber, 1999; Durban and Elston, 2005). Mathematical models can incorporate the dynamics of an open population. This is called population dynamics modeling and the goal is to predict the future estimate of animal abundance which aids the decision making process.

Population Growth Models

Population growth model is usually concerned with four important parameters: birth, death, immigration and emigration (White, 2000). A population-growth model which is independent of the population density can be represented by a simple difference equation of the form

$$n_{t+1} = n_t \ (1 + r), \tag{2.4}$$

where n_t can be the number of animals in a day,month or year and

$$r = \frac{(\text{birth} - \text{death}) + (\text{immigration} - \text{emigration})}{\text{time}} \ .$$

Thus, population growth rate can be given by

$$\lambda = \frac{n_{t+1}}{n_t} = 1 + r \ . \tag{2.5}$$

In case that the time scale unit is years then the Equation (2.5) gives the annual growth rate and $\lambda < 1$ would indicate a decreasing population. Furthermore, the model in Equation (2.4) can be made more realistic by making it density dependent because it exhibits exponential population growth. Furthermore, animal populations depend on the resources (food, water) available in their shared habitat and only a sufficient amount of resources promise a steady growth in the population size. This implies that the population growth is a function of the population size

$$r(n_t) = r_0(1 - \frac{n_t}{k}), \tag{2.6}$$

where k is known as the carrying capacity and r_0 is the maximum growth rate for an extremely small population size. The carrying capacity is a property of the environment; it is the maximum limit in terms of population size that an environment can support without constant degradation of the resources. Substituting expression in Equation (2.6) to the model Equation (2.4) gives

$$n_{t+1} = n_t[1 + r_0(1 - \frac{n_t}{k})] \ . \tag{2.7}$$

The models in Equation (2.4) and Equation (2.7) can also be represented with differential equations for the continuous time case but animal populations exhibit discrete birth pulses. Therefore, we restrict our discussion to only discrete time cases.

Age Based Models

Another form of population models known as age-structured models tend to be more complex but at the same time they can be more realistic. In age-structured population models the parameters of birth and death can be replaced by survival (mortality) and reproduction (fertility) parameters. Again age-structured population models can be formulated both as density independent age-structure models or density dependent age-structure models with the lateral being more realistic and more complex. A famous formulation of age-structured models in the form of matrices was given by (Leslie, 1945). The Leslie Matrix population model is used to determine the growth of a population, as well as the age distribution with in the population over time. The Leslie Matrix population model is given as

$$\boldsymbol{n}_{t+1} = \boldsymbol{A}\boldsymbol{n}_t, \tag{2.8}$$

where $\boldsymbol{n}_t$ is a vector with components representing the number of individuals in each age group at time t and $\boldsymbol{A}$ is the Leslie matrix. The model in matrix formulation is given as

$$\begin{bmatrix} n_1 \\ n_2 \\ n_3 \\ \vdots \\ n_{a-1} \end{bmatrix}_{t+1} = \begin{bmatrix} b_1 & b_2 & b_3 & \dots & b_{a-1} & b_a \\ s_1 & 0 & 0 & \dots & 0 & 0 \\ 0 & s_2 & 0 & \dots & 0 & 0 \\ 0 & 0 & s_3 & . & \vdots & \vdots \\ \vdots & \vdots & . & \ddots & . & \vdots \\ 0 & 0 & 0 & \dots & s_{a-1} & 0 \end{bmatrix} \begin{bmatrix} n_1 \\ n_2 \\ n_3 \\ \vdots \\ n_{a-1} \end{bmatrix}_{t}, \tag{2.9}$$

where $b_i : i = 1, 2, \dots, a$ is the fertility(number of offspring) of a female of age i, $s_i : i = 1, 2, \dots, a-1$ is the survival probability that an individual of age i at time t will survive to time $t + 1$ and a is the maximum age limit of the particular animal.

Process Variation

Animal population dynamics models need to be stochastic rather deterministic because animal population growth and reduction involves uncertainty due to latent natural processes. This phenomenon is termed as process variation (Thompson et al., 1998; White, 2000) and there can be many reasons for process variation:

- Demographic variation which is the uncertainty in the expectation of the survival and reproduction of an animal. Demographic variation can lead to extinction in very small populations but has less effect on large populations.

- Temporal variation, for example, change in the weather intensity from year to year can lead to variation in survival and reproduction.
- Spatial variation refers to geological changes in the habitat of animals which may cause changes in resources, for example, different areas having different amount of rainfall. This again leads to variation in survival and reproduction.
- Process variations on an individual level, for example, different animals can survive and reproduce differently because of different genes. This can also be called genetic variation.

On the other hand the uncertainty in the measurements of the estimation methods is termed as sampling variation. It has been widely acknowledged in literature that the state-space modeling framework provides a suitable method for incorporating both stochastic processes and observation uncertainty in to population dynamics models (Buckland et al., 2004b, 2007).

2.2.3 State-space Models of Animal Population

State-space models of animal population constitute discrete-time models usually with finite number of states. The models can be deterministic or stochastic depending on the state process model and observation model. For population dynamics state-space models can be given in a probabilistic notation as

$$\begin{aligned} \boldsymbol{n}_0 &\sim p(\boldsymbol{n}_0|\theta) \\ \boldsymbol{n}_t &\sim p(\boldsymbol{n}_t|\boldsymbol{n}_{t-1},\theta) \\ \boldsymbol{y}_t &\sim p(\boldsymbol{y}_t|\boldsymbol{n}_t,\theta), \end{aligned} \tag{2.10}$$

where

- $p(\boldsymbol{n}_t|\boldsymbol{n}_{t-1},\theta)$ is the population dynamics model or state process distribution.
- $p(\boldsymbol{y}_t|\boldsymbol{n}_t,\theta)$ is the observation model or observation process distribution.
- $\boldsymbol{n}_t$ is known as the state vector at time t.
- $\boldsymbol{y}_t$ is the observation vector at time t.
- $p(\boldsymbol{n}_0|\theta)$ is the prior state distribution

The state vector can include components such as individual counts, age groups, stages of a life-cycle, genotypes and some other demographics. The observation or measurement vector consist of the counts from any sampling method, for example, census or survey.

Bayesian inference methods such as Markov chain Monte Carlo (MCMC) and Sequential Importance Sampling (SIS) have been used to estimate the state of the population where the models have a state-space framework (Newman et al., 2009; Buckland et al., 2004b, 2007). A well known software application for applying Bayesian inference to population dynamics models is the WinBUGS package (Gimenez et al., 2009). Other recursive filtering methods such as the Kalman filter has also been used for estimation of state-space models in animal ecology (Newman, 1998).

2.2.4 State-space Models of Animal Movement

Animal spatial distribution is usually a fundamental part of animal abundance studies. Population dynamics models have been embedded with movement information described by distributions of movement rates and directions. An example of a state-space model describing the mortality and movement of Pacific coho salmon is given in (Newman, 1998)

$$\boldsymbol{n}_t = \boldsymbol{M}_t \boldsymbol{S}_t \boldsymbol{n}_{t-1} + \boldsymbol{w}_t \qquad \boldsymbol{w}_t \sim \mathrm{N}(0, \boldsymbol{\Sigma}_{w_t}) \tag{2.11a}$$

$$\boldsymbol{c}_t = \boldsymbol{H}_t \boldsymbol{n}_t + \boldsymbol{v}_t \qquad \boldsymbol{v}_t \sim \mathrm{N}(0, \boldsymbol{\Sigma}_{v_t}), \tag{2.11b}$$

where $\boldsymbol{n}_t$ is the unobserved state process vector which consists of animal counts by area, $\boldsymbol{c}_t$ is the observed measurement vector which consists of salmon catches at time (t) and $\boldsymbol{M}_t, \boldsymbol{S}_t, \boldsymbol{H}_t$ are movement, survival and harvest matrices respectively.The components of $\boldsymbol{M}_t$ consist of the individual area to area movement probabilities. $\boldsymbol{S}_t$ is a diagonal matrix with elements giving the expected survival probabilities and $\boldsymbol{H}_t$ is also a diagonal matrix of harvest(observation) rates. $\boldsymbol{v}_t$ and $\boldsymbol{w}_t$ are zero mean Gaussian noise vectors with covariance matrices $\boldsymbol{\Sigma}_{w_t}$ and $\boldsymbol{\Sigma}_{v_t}$.

Constructing animal movement models in order to predict the spacial pattern that an animal or group of animals can produce is known as Eulerian method (Smouse et al., 2010). Eulerian approaches rely on diffusion models and place-based information. On the other hand the classic individual-based approach to modeling animal movement is by using stochastic differential equations (SDE) (Brillinger et al., 2002; Preisler et al., 2004). This method of modeling is known as the Lagrangian approach (Smouse et al., 2010). An example SDE model of animal movement at time t and location $\boldsymbol{r}(t)$ is given as

$$\begin{bmatrix} d\boldsymbol{x}(t) \\ d\boldsymbol{y}(t) \end{bmatrix} = \begin{bmatrix} \mu_x\{\boldsymbol{r}(t), t\} \\ \mu_y\{\boldsymbol{r}(t), t\} \end{bmatrix} dt + \boldsymbol{D}\{\boldsymbol{r}(t), t\} \begin{bmatrix} d\boldsymbol{\Psi}_x(t) \\ d\boldsymbol{\Psi}_y(t) \end{bmatrix}, \tag{2.12}$$

where

- $\boldsymbol{dx}(t)$ and $\boldsymbol{dy}(t)$ are incremental step sizes in the (x, y) co-ordinates.
- $\boldsymbol{\mu} = (\mu_x, \mu_y)^T$ consists of the drift parameters.
- $\boldsymbol{D}$ is the diffusion matrix which gives correlation between x and y directions over time.
- $\boldsymbol{\Psi}_x$ and $\boldsymbol{\Psi}_y$ are zero mean random processes.

The drift parameters control the direction, where as the diffusion parameters are responsible for the speed of motion. There are a few special cases that arise from the model in Equation (2.12) (Preisler et al., 2004).

1. The drift term is zero
    - and the diffusion terms are independent along (x, y) co-ordinates. This motion is an uncorrelated random walk.
    - and the diffusion terms are not independent. This motion is a correlated random walk (CRW).
2. The drift term is non-zero
    - and the diffusion terms are independent along (x, y) co-ordinates. This motion is a biased random walk in the direction of the drift parameters.
    - and it is directed towards a single point, and the diffusion terms are independent. This motion is a special case known as the mean-reverting Ornstein-Uhlenbeck (O-U) process.

An important feature in modeling animal population dynamics is learning about the home range behavior and individual habitat. Although some aspects of animal movement, for example, relocation can be observed from survey data (e.g; Mark-recapture) and then statistically modeled as probability distributions by embedding the distributions into state-space models, survey type sampling data is unable to provide dense positional data.

Radio tagging and GPS telemetry data have enabled researchers to observe animal movements at a finer scale and adequately understand phenomena such as foraging and home range behavior (Börger et al., 2008). Radio tagging and GPS telemetry data can be distorted by observational errors. Therefore, state-space models have been used as an effective method of finding the relationship between stochastic dynamics models of movement and uncertain observations (Patterson et al., 2008). A state-space model of individual animal movement can be written as

$$\begin{aligned} \boldsymbol{x}_t &= g(\boldsymbol{x}_{t-1}, \eta_{t-1}) \\ \boldsymbol{y}_t &= h(\boldsymbol{x}_t, \varepsilon_t), \end{aligned} \tag{2.13}$$

where

- $\boldsymbol{x}_t$ is the state vector with components such as position, direction or turn angle and speed of the animal at time t.
- $\boldsymbol{y}_t$ is the observation vector at time t (e.g. position).
- $g()$ is the population dynamics model.
- $h()$ is the observation model.
- η_{t-1} is the process noise.
- ε_t is the observation noise.

A few example applications of these models can be found in (Anderson-Sprecher and Ledolter, 1991; Nielsen et al., 2006; Royer et al., 2005).

2.3 Bayesian Optimal Filtering

The approach used in this thesis for estimating the population of large carnivores is called multiple target tracking. Multiple target tracking is an application area of Bayesian optimal filtering methods. It must be noted that the standard approaches discussed earlier in this chapter were more focused on sampling techniques and mathematical models while this section presents the dynamic estimation methods which have been widely used especially in the case of state-space models. We present the general equations of Bayesian optimal filtering in this section and the more specialized algorithms in the remaining sections of this chapter.

The methodology for recursively estimating the states of a dynamic system from the Bayesian inference point of view is known as Bayesian optimal filtering. Consider the following state-space model in probabilistic notation (Doucet et al., 2001; Ristic et al., 2004)

$$\begin{aligned} \boldsymbol{x}_k &\sim p(\boldsymbol{x}_k | \boldsymbol{x}_{k-1}) \\ \boldsymbol{y}_k &\sim p(\boldsymbol{y}_k | \boldsymbol{x}_k), \end{aligned} \tag{2.14}$$

where $\boldsymbol{x}_k$ is the hidden state vector of the dynamics model and $\boldsymbol{y}_k$ is the observed measurement vector.

The goal of Bayesian optimal filtering is to construct the posterior distribution $p(\boldsymbol{x}_k|\boldsymbol{y}_{1:k})$ of the state $\boldsymbol{x}_k$ given all the measurements $\boldsymbol{y}_{1:k}$ observed up to time step k. The recursive estimation starts with defining the prior distribution $\boldsymbol{x}_0 \sim p(\boldsymbol{x}_0)$ for initializing the filtering process and the subsequent optimal filtering equations also known as Bayesian filtering equations are given as

$$p(\boldsymbol{x}_k|\boldsymbol{y}_{1:k-1}) = \int p(\boldsymbol{x}_k|\boldsymbol{x}_{k-1})\ p(\boldsymbol{x}_{k-1}|\boldsymbol{y}_{1:k-1})\ d\boldsymbol{x}_{k-1} \tag{2.15a}$$

$$p(\boldsymbol{x}_k|\boldsymbol{y}_{1:k}) = \frac{1}{\boldsymbol{Z}_k}\ p(\boldsymbol{y}_k|\boldsymbol{x}_k)\ p(\boldsymbol{x}_k|\boldsymbol{y}_{1:k-1}) \tag{2.15b}$$

where the normalization constant is given as

$$\begin{aligned}\boldsymbol{Z}_k &= p(\boldsymbol{y}_k|\boldsymbol{y}_{1:k-1}) \\ &= \int p(\boldsymbol{y}_k|\boldsymbol{x}_k)\ p(\boldsymbol{x}_k|\boldsymbol{y}_{1:k-1})\ d\boldsymbol{x}_k\end{aligned}$$

Equation (2.15a) is known as the Chapman-Kolmogorov equation which defines the prediction step that propagates the posterior distribution of the state from time step $k-1$ to k. The recursion is started from the prior distribution $p(\boldsymbol{x}_0|\boldsymbol{y}_{1:0}) \triangleq p(\boldsymbol{x}_0)$. Subsequently at time step $k > 0$ the prior distributions $p(\boldsymbol{x}_k|\boldsymbol{y}_{1:k-1})$ can be obtained by numerical integration over the dynamics model $p(\boldsymbol{x}_k|\boldsymbol{x}_{k-1})$ and the posterior of the previous step $p(\boldsymbol{x}_{k-1}|\boldsymbol{y}_{1:k-1})$. Equation (2.15b) is obtained by applying the Bayes rule that gives the marginal posterior distribution $p(\boldsymbol{x}_k|\boldsymbol{y}_{1:k})$ of the state vector $\boldsymbol{x}_k$ at $k > 0$. This is the update step and the posterior distribution is updated with the current observation $\boldsymbol{y}_k$. $\boldsymbol{Z}_k$ is the normalizing denominator and $p(\boldsymbol{y}_k|\boldsymbol{x}_k)$ is the measurement likelihood.

2.3.1 Kalman Filter

A closed form solution to the Bayesian optimal filtering problem with the assumption that the model is discrete-time linear Gaussian is known as the Kalman Filter. Approximations of the target state distributions are dispensable because the result of Kalman filtering is exactly Gaussian due to the linear Gaussian model assumption (Särkkä, 2006). However, non-linear models and Gaussian noise can be estimated using the extended Kalman filter (EKF) or the unscented Kalman filter (UKF). The idea in EKF is that the non-linearity is dealt with by using linearization and the model is formulated again as a linear Gaussian model. The UKF solves the same problem by approximating the mean and covariance of non-linear functions of the Gaussian random variables in the model by propagating a set of sigma-points through the non-linear functions (Julier and Uhlmann, 2004). A linear Gaussian state-space model can be written in probabilistic notation as

$$\begin{aligned} p(\boldsymbol{x}_k|\boldsymbol{x}_{k-1}) &\sim \mathrm{N}(\boldsymbol{x}_k|\boldsymbol{A}_{k-1}\boldsymbol{x}_{k-1}, \boldsymbol{Q}_k) \\ p(\boldsymbol{y}_k|\boldsymbol{x}_k) &\sim \mathrm{N}(\boldsymbol{y}_k|\boldsymbol{H}_k\boldsymbol{x}_k, \boldsymbol{R}_k). \end{aligned} \tag{2.17}$$

A more common notation used to represent linear Gaussian models in dynamic estimation literature is

$$\begin{aligned} \boldsymbol{x}_k &= \boldsymbol{A}_{k-1}\boldsymbol{x}_{k-1} + \boldsymbol{q}_{k-1} \\ \boldsymbol{y}_k &= \boldsymbol{H}_k\boldsymbol{x}_k + \boldsymbol{r}_k, \end{aligned} \tag{2.18}$$

where $\boldsymbol{x}_k$ is the state, $\boldsymbol{y}_k$ is the measurement, $\boldsymbol{q}_{k-1} \sim \mathrm{N}(0, \boldsymbol{Q}_{k-1})$ is the process noise and $\boldsymbol{r}_k \sim \mathrm{N}(0, \boldsymbol{R}_k)$ is the measurement noise. $\boldsymbol{A}_{k-1}$ is the transition matrix and $\boldsymbol{H}_k$ is the measurement model matrix.

The recursive algorithmic steps required to estimate the states at each time step k are given in Algorithm 2.3.1. The Kalman filter is first initialized and the initial state is given by a Gaussian prior distribution of the form

$$\boldsymbol{x}_0 \sim \mathrm{N}(\boldsymbol{m}_0, \boldsymbol{P}_0) \ , \tag{2.19}$$

where $\boldsymbol{m}_0$ is the initial mean and $\boldsymbol{P}_0$ is the initial covariance.

Algorithm 2.3.1 : Kalman filter

```
Prediction step:
    $\boldsymbol{m}_k^- = \boldsymbol{A}_{k-1}\boldsymbol{m}_{k-1}$
    $\boldsymbol{P}_k^- = \boldsymbol{A}_{k-1}\boldsymbol{P}_{k-1}\boldsymbol{A}_{k-1}^T + \boldsymbol{Q}_{k-1}$
Update step:
    $\boldsymbol{v}_k = \boldsymbol{y}_k - \boldsymbol{H}_k\boldsymbol{m}_k^-$
    $\boldsymbol{S}_k = \boldsymbol{H}_k\boldsymbol{P}_k^-\boldsymbol{H}_k^T + \boldsymbol{R}_k$
    $\boldsymbol{K}_k = \boldsymbol{P}_k^-\boldsymbol{H}_k^T\boldsymbol{S}_k^{-1}$
    $\boldsymbol{m}_k = \boldsymbol{m}_k^- + \boldsymbol{K}_k\boldsymbol{v}_k$
    $\boldsymbol{P}_k = \boldsymbol{P}_k^- - \boldsymbol{K}_k\boldsymbol{S}_k\boldsymbol{K}_k^T$
```

2.3.2 Particle Filtering

Particle filtering uses sequential Monte Carlo methods to solve the Bayesian optimal filtering problem. Particle filters can be used to solve a wide range of non-linear and non-Gaussian noise filtering problems since the method is based on approximating the posterior distribution of the state variables via Monte Carlo. The posterior distribution $p(\boldsymbol{x}_k|\boldsymbol{y}_{1:k})$ of the state $\boldsymbol{x}_k$ at time step k is approximated as a set of weighted Monte Carlo samples $\{(w_k, \boldsymbol{x}_k^{(i)}) : i = 1, \ldots, N\}$. The samples are drawn from an importance distribution which approximates the target posterior distribution at each step.

Earlier algorithms of particle filtering known as sequential importance sampling (SIS) suffered from the problem of degeneracy. This means that in certain conditions almost all the particles have zero weights and only a few are non-zero. This problem can be solved by introducing an additional resampling step to the SIS and in this case the algorithm is known as sequential importance resampling (SIR) (Ristic et al., 2004). The idea is to draw N new samples from a discrete distribution defined by the weights and replace the old samples. Usually resampling is performed when it is actually needed. One way of achieving this is by computing the effective number of particles (samples) at each step and resampling if the effective number of particles are less then a predefined threshold. This is termed as *adaptive resampling* which actually consists of other methods as well like resampling after a predefined interval. The effective number of particles can be calculated as

$$n_{EFF} = \frac{1}{\sum_{i=1}^{N} (w_k^{(i)})^2}, \tag{2.20}$$

where $w_k^{(i)}$ is the normalized weight of particle i at time step k. Resampling can be performed, for example, when $n_{EFF} < N/10$ where N is the total number of particles.

The performance of the SIR is highly dependent on the method of constructing the importance distribution. The optimal importance distribution in terms of variance is (Doucet et al., 2001; Ristic et al., 2004).

$$\pi(\boldsymbol{x}_k|\boldsymbol{x}_{k-1}, \boldsymbol{y}_{1:k}) = p(\boldsymbol{x}_k|\boldsymbol{x}_{k-1}, \boldsymbol{y}_k). \tag{2.21}$$

In case the optimal distribution has a form that sampling from it directly is unfeasible then methods of linearisation can be used, for example, EKF, UKF or other non-linear forms of the Kalman filter. The simplest form of SIR is the *bootstrap filter* which uses the dynamic model $p(\boldsymbol{x}_k|\boldsymbol{x}_{k-1})$ as the importance distribution. The algorithm for the bootstrap filter is given in Algorithm 2.3.2. Due to an inefficient importance distribution the bootstrap filter normally requires a large number of Monte Carlo samples for accurate estimation. The resampling is usually performed at each step. Another pitfall in SIR is the sample impoverishment problem which means that only a few samples that have large weights get replicated.

Algorithm 2.3.2 : Bootstrap filter

```
1: For each sample $\{\boldsymbol{x}_{k-1}^{(i)}, i = 1, \ldots, N\}$, draw new $\boldsymbol{x}_k^{(i)}$ from
   the dynamics model:
       $\boldsymbol{x}_k^{(i)} \sim p(\boldsymbol{x}_k | \boldsymbol{x}_{k-1}^{(i)}), \quad i = 1, \ldots, N.$
2: Calculate the weights
       $w_k^{(i)} = p(\boldsymbol{y}_k | \boldsymbol{x}_k^{(i)}), \quad i = 1, \ldots, N.$
3: Normalize weights to sum to unity.
4: Perform resampling.
```

2.3.3 Rao-Blackwellized Particle Filtering

Sometimes it is possible to disintegrate the Bayesian filtering problem in to subproblems, for example, estimation of a linear Gaussian part and approximation of a non-linear part. The linear Gaussian part can be solved analytically, for example by using the Kalman filter and the non-linear part can be solved by particle filtering. The extended Kalman filter can also be used in case of slight non-linearities. This idea of marginalizing the states of the dynamic system is known as Rao-Blackwellization. The Rao-Blackellization improves the efficiency of the normal SIR by reducing the number of Monte-Carlo samples required to approximate the target distribution. This generates estimators with less variance as compared to standard Monte Carlo sampling (Doucet et al., 2001; Ristic et al., 2004).

Rao-Blackwellized filtering can be used for state estimation of conditionally Gaussian Markov models,

$$\begin{aligned} p(\boldsymbol{x}_k | \boldsymbol{x}_{k-1}, \lambda_{k-1}) &= \mathrm{N}(\boldsymbol{x}_k | \boldsymbol{A}_{k-1}(\lambda_{k-1}) \boldsymbol{x}_{k-1}, \boldsymbol{Q}_{k-1}(\lambda_{k-1})) \\ p(\boldsymbol{y}_k | \boldsymbol{x}_k, \lambda_k) &= \mathrm{N}(\boldsymbol{y}_k | \boldsymbol{H}_k(\lambda_k) \boldsymbol{x}_k, \boldsymbol{R}_k(\lambda_k)) \\ p(\lambda_k | \lambda_{k-1}) &= \text{(any given form)}, \end{aligned} \tag{2.22}$$

where $\boldsymbol{x}_k$ is the state, $\boldsymbol{y}_k$ the measurement, and λ_k an arbitrary latent variable. If the prior distribution of $\boldsymbol{x}_k$ is also Gaussian the state variables $\boldsymbol{x}_k$ can be integrated out in closed form and only the latent variables λ_k need to be sampled. The Algorithm 2.3.3 shows the recursive steps required for marginalized filtering of the model in Equation (2.22). The result of the Rao-Blackwellized particle filter (RBPF) can be represented with an approximation density of the form

$$p(\boldsymbol{x}_k, \lambda_k | \boldsymbol{y}_{1:k}) \approx \sum_{i=1}^{N} w_k^{(i)} \; \delta(\lambda_k - \lambda_k^{(i)}) \; \mathrm{N}(\boldsymbol{x}_k | \boldsymbol{m}_k^{(i)}, \boldsymbol{P}_k^{(i)}).$$

Algorithm 2.3.3 : Conditionally Gaussian Rao-Blackwellized particle filter

```
1: Kalman filter prediction:
   Compute all means and covariances based on the previous drawn latent variable $\lambda_{k-1}^{(i)}$ for each particle $i = 1, \ldots, N$
       $\boldsymbol{m}_k^{-(i)} = \boldsymbol{A}_{k-1}(\lambda_{k-1}^{(i)})\boldsymbol{m}_{k-1}^{(i)}$
       $\boldsymbol{P}_k^{-(i)} = \boldsymbol{A}_{k-1}(\lambda_{k-1}^{(i)})\boldsymbol{P}_{k-1}^{(i)}\boldsymbol{A}_{k-1}^T(\lambda_{k-1}^{(i)}) + \boldsymbol{Q}_{k-1}(\lambda_{k-1}^{(i)})$
2: Draw new variables $\lambda_k^{(i)}$ for each particle in $i = 1, \ldots, N$ from the corresponding importance distributions
       $\lambda^{(i)k} \sim \pi(\lambda_k | \lambda_{1:k-1}^{(i)}, \boldsymbol{y}_{1:k})$
3: Calculate new (unnormalized) weights as follows:
       $w_k^{(i)} \propto w_{k-1}^{(i)} \frac{p(\boldsymbol{y}_k | \lambda_{1:k}^{(i)}, \boldsymbol{y}_{1:k-1}) p(\lambda_k^{(i)} | \lambda_{k-1}^{(i)})}{\pi(\lambda_k | \lambda_{1:k-1}^{(i)}, \boldsymbol{y}_{1:k})}$
   where the likelihood term is the marginal measurement likelihood of the Kalman filter such that the model parameters in the Kalman filter are conditioned on the drawn variable value $\lambda_k^{(i)}$
       $p(\boldsymbol{y}_k | \lambda_{1:k}^{(i)}, \boldsymbol{y}_{1:k-1}) = \mathrm{N}\Big(\boldsymbol{y}_k | \boldsymbol{H}_k(\lambda_k^{(i)})\boldsymbol{m}_k^{-(i)}, \boldsymbol{H}_k(\lambda_k^{(i)})\boldsymbol{P}_k^{-(i)}\boldsymbol{H}_k^T(\lambda_k^{(i)}) + \boldsymbol{R}_k(\lambda_k^{(i)})\Big).$
   Then normalize the weights to sum to unity.
4: Kalman filter update:
   Perform update based on the drawn latent variables $\lambda_k^{(i)}$
       $\boldsymbol{v}_k^{(i)} = \boldsymbol{y}_k - \boldsymbol{H}_k(\lambda_k^{(i)})\boldsymbol{m}_k^-$
       $\boldsymbol{S}_k^{(i)} = \boldsymbol{H}_k(\lambda_k^{(i)})\boldsymbol{P}_k^{-(i)}\boldsymbol{H}_k^T(\lambda_k^{(i)}) + \boldsymbol{R}_k(\lambda_k^{(i)})$
       $\boldsymbol{K}_k^{(i)} = \boldsymbol{P}_k^{-(i)}\boldsymbol{H}_k^T(\lambda_k^{(i)})\boldsymbol{S}_k^{-1}$
       $\boldsymbol{m}_k^{(i)} = \boldsymbol{m}_k^{-(i)} + \boldsymbol{K}_k^{(i)}\boldsymbol{v}_k^{(i)}$
       $\boldsymbol{P}_k^{(i)} = \boldsymbol{P}_k^{-(i)} - \boldsymbol{K}_k^{(i)}\boldsymbol{S}_k^{(i)}[\boldsymbol{K}_k^{(i)}]^T$
5: If the effective number of particles is too low, perform resampling
```

2.4 Target Tracking and Data Association

Target tracking is an application area of Bayesian optimal filtering. Target tracking in abstract form has its origin in estimation theory (Bar-Shalom et al., 2001). The definition of target tracking is case-dependent and it is based upon the type of solution required to solve the underlying problem. Target tracking, in general, can be defined as estimation of the state of a moving object (target) from noisy measurements. Measurements are obtained from a single sensor or multiple sensors which can be at fixed locations or moving platforms (Bar-Shalom and Li, 1995). Target tracking is further classified to single target tracking and multiple target tracking. The Figure 2.1 shows single target tracking with a single sensor and the Figure 2.2 shows single target tracking with multiple sensors. In case of both multiple targets and multiple sensors as shown in Figure 2.3, the measurements need to be combined and this is generally known as sensor fusion.

Usually, the state of a target consists of the position and velocity of the object, and sometimes acceleration of the target. The state is observed through measurements obtained from different sources depending on the application of interest. Measurements can have different types of sources such as acoustic, radar, video or signals obtained from some sensor, furthermore, the measurements can be noisy. Once these measurements are obtained, they are either used in raw form or preprocessed before the application of any estimation method. Classical applications of target tracking consist of flight control systems, remote surveillance, moving vehicle tracking and navigation.

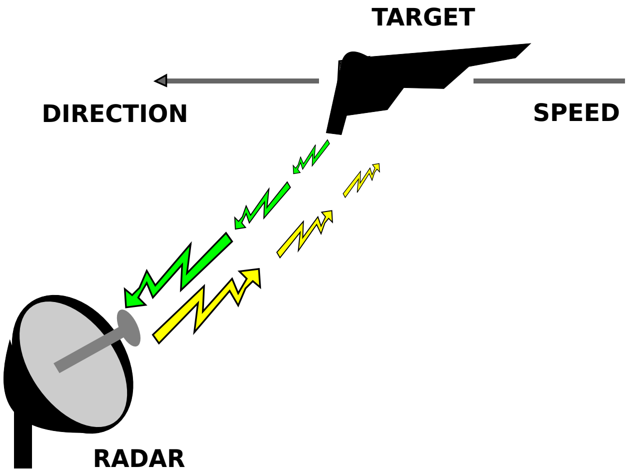

Figure 2.1: Single target tracking with a single sensor

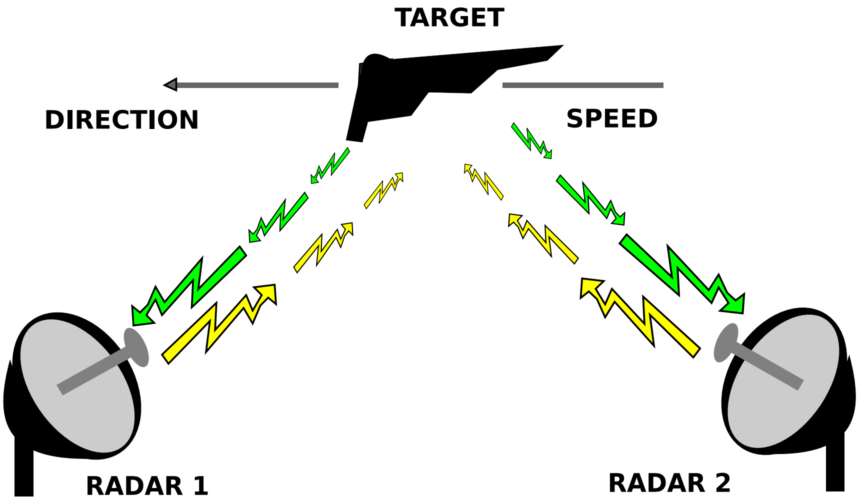

Figure 2.2: Single target tracking with multiple sensors

A more complex problem occurs when there are multiple targets moving in the same geographical area. This requires a solution that, in addition to tracking targets, can also determine which measurement originated from which target, commonly known as data association. The basic difference in methodologies for multiple target tracking is the implementation of the data association process. There are many data association approaches used in multiple target tracking; these include very simple nearest neighbor approaches to the very complex multiple hypothesis tracking (MHT).

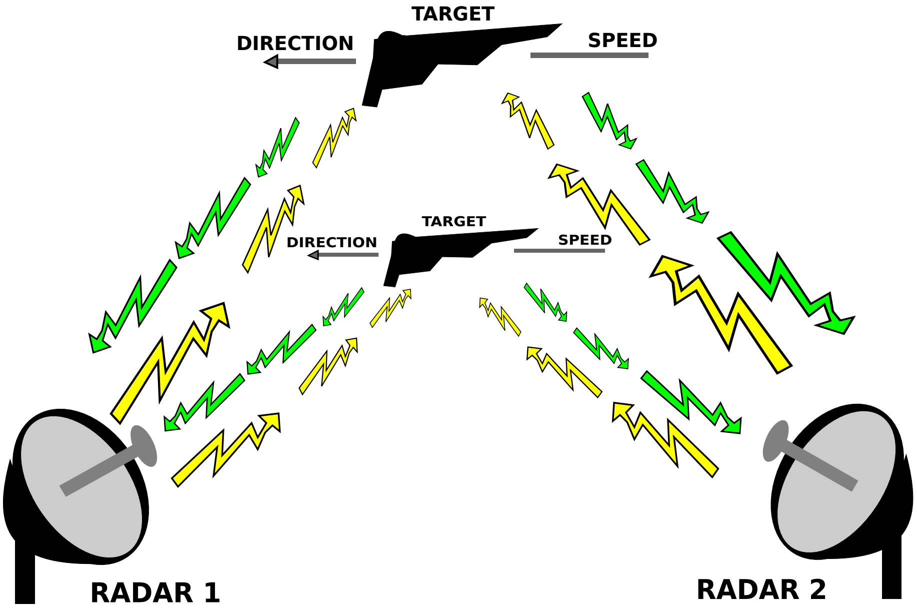

Figure 2.3: Multiple target tracking with multiple sensors

A well-known approach to data association is the global nearest neighbor (GNN) method also known as single most probable hypothesis tracking (Blackman and Popoli, 1999). GNN consists of two important steps referred to as gating and association. Gating is the process of eliminating the most unlikely target-to-measurement pairings (associations). The association process is simple when there is a single measurement gated to each target. However, conflicts arise when multiple measurements arise in a single gate or same measurement duplicates in different gates. These cases are generally resolved using an assignment matrix. The GNN algorithm uses the measurements closest to a predicted target for updating the state parameters of that target and remaining measurements are discarded. Another nearest neighbor approach is the strongest-neighbor filter (SNF). The SNF algorithm keeps the signal with the highest intensity among the validated measurements in the gate while others are discarded.

The above mentioned approaches are similar in the sense that they use a single measurement for target updates while all the other measurements are discarded. An alternative to this approach is that all of the measurements are used with different weights (probabilities) for target updates, this is known as probabilistic data association. Probabilistic data association filter (PDAF) is a method which consists of the probabilities for all validated measurements corresponding to the targets of interest(Kirubarajan and Bar-Shalom, 2005). Joint PDA is another extension of the PDA approach where the measurement-to-track association probabilities are evaluated and combined to find the state estimate (Bar-Shalom and Li, 1995). Usually in all multiple target tracking problems the 'number of targets' is unknown, therefore, the data association approach used must determine the number of targets in addition to data association of the targets. A number of approaches have also been proposed for such kind of problems (Blackman and Popoli, 1999; Bar-Shalom et al., 2001).

Another important component of the state of a moving target especially in case of multiple targets can be the attribute measurements (Bar-Shalom, 1987). It is often very difficult to determine which measurement is generated by which target if the identities of the individual targets are unknown and the measurements obtained have only kinematic components. Attributes or features of the targets that can be obtained are highly dependent on the capabilities of the source of measurement. Sensors that can obtain imagery information of the targets at a certain resolution are able to distinguish between targets based on their shape, size or color, for example, a vehicle tracking system using satellite imagery technology can classify vehicles in to different categories (e.g., car, truck, tractor). However, more restricted sources that can only obtain kinematic measurements can use prior information about the targets, for example, the maximum speed a target can attain or the maximum turning angle possible. This is known as coarse kinematic information (Blackman and Popoli, 1999). In case the coarse kinematic information is also similar among all the targets then the data association process becomes even more difficult.

Chapter 3

Materials, Models and Methods

3.1 Data Sources

We have used an unconventional method of estimating animal abundance in comparison to the standard methodology. This is mainly due to an unusual data collection process. The data collection process is based on a reporting procedure that involves multiple observers. The observations can be registered through websites, phones or district game management offices. This is a voluntary task which can be performed by anybody in Finland, for example, it is possible that somebody traveling via car observes a carcass of a dead animal and reports to the district game management office. The whole dataset consists of observations collected from almost every district of Finland. This data collection is a continuous process which is supervised by the *Finnish Game and Fisheries Research Institute.*

The dataset comprises mainly of four large carnivores: brown bear, wolf, lynx and wolverine. The dataset also consists of index based data which is considered to be more reliable information. The field work required to collect index based samples is also a voluntary effort of around 1500 hunters all around Finland. These volunteers have exceptional skill in finding and identifying marks left behind by the animals. The observations are based on both direct sighting of the animal and its remains (field-signs). Field-signs mainly consist of foot-prints, carcasses of dead animal or prey, feces and habitual structures. One of the more important descriptors in the data set is the number of cubs and one year olds which are assumed to be following their mother. The foot print observations are also used to determine the litter size and age of the animals. We briefly present the biological information and animal tracks description that aid in the estimation of animal population.

Brown Bear

A litter of $1-3$ and at times 4 cubs is born between January to March during the hibernation period of a female bear. The cubs tend to follow the mother before hibernating again the following winter and usually leave their mother in late spring or summer of the next year. Males tend to disperse from their natal areas whereas females usually establish home ranges nearby or overlapping their natal areas. Brown bears are solitary animals and usually live their whole life in a single but large habitual region. The home ranges of male bears are larger than those of female bears. The annual home range of a female can be $60-300$ square kilometers while that of a male can be over 1000 square kilometers (Katajisto, 2006).

Brown bears hibernate for $4-5$ months which restricts the reliable sampling period to merely $5-6$ months. Due to the long winter sleep a bear has to consume sufficient food during spring and summer. This makes bears very active and they tend to move around $10-30$ kilometers a day in search of food. Bear foot prints can be found quite apparently on sand and moss due to the huge weight of the animal. Foot prints also assist in identifying other field signs for the presence of a bear such as broken tree branches, droppings and excavated anthills. Figure 3.1 shows a brown bear[1] and the foot print; the front foot or paw is $12-15$cm in length and $10-18$cm in width while the rear foot is $18-25$cm in length and $10-18$cm in width.

Figure 3.1: Brown bear and foot sizes

Wolf

More often a pack of wolves is formed around a breeding alpha pair or the dominant pair. Other members of the pack are usually $1-2$ year olds of the same family.

---

[1] By Hillebrand, Steve [Public domain], via Wikimedia Commons. http://creativecommons.org/licenses/by-sa/3.0/

The female usually gives birth to a litter of $3-6$ cubs per year. The cubs are blind and deaf when born and are nursed by the mother in a den for the first three weeks. Wolves are highly social animals. All members of the pack hunt together and help looking after the cubs . At the age of $1-2$ years the young might leave the pack and travel far from their birth place in search of their own territory and partner. Wolf territories vary between $100-1000$ square kilometers. The territories are well marked and strongly defended against other packs (Salvatori and Linnell, 2005).

Wolves travel $30-50$ kilometers a day but can also travel 160 kilometers if food is scarce. Reliable descriptors for sampling are observations and field signs of wolf packs rather than single observations since a single wolf is very hard to track unless radio or GPS telemetry is used. Wolves move along roads, paths and tracks made by humans and other animals. Their foot prints resemble to that of dogs but can easily be distinguished by size and the tracks often tend to be in a straight path. Figure 3.2 shows a wolf[2] and the foot print; the length of the foot is $9-10$cm while the width is $6.5-10$cm.

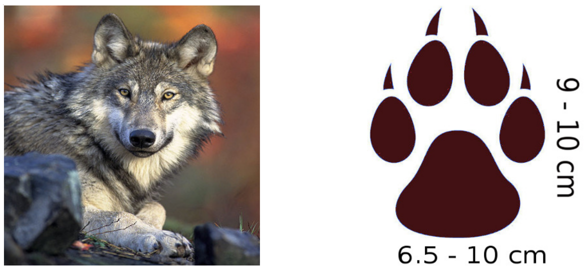

Figure 3.2: Wolf and foot size

Lynx

A female lynx usually gives birth to a litter of $2-3$ kittens and more rarely 1 or 4 kittens are born. The lair is usually a hallow place with constant temperature since the kittens are unable to regulate their body temperatures. The young begin eating solid food only when they are at least three months old while they keep suckling their mother for up to six months. Then the kittens leave the lair and start following the mother. Initially unable to hunt they practice at prey captured by the mother but learn rapidly and soon join the actual hunting. Lynx are solitary animals

---

[2] By Gary Kramer [Public domain], via Wikimedia Commons. http://creativecommons.org/licenses/by-sa/3.0/

except during the mating season which usually starts at the end of February to the early April. Females usually give birth in May-June. The young might stay with the mother at most for one year before dispersing. The home range and behavior of lynx varies from region to region and primarily depends on the landscape and density of prey (Breitenmoser, 2000). Generally, males travel more than females and have larger home ranges that can vary from 120 to 1600 square kilometers. Females with kittens can have a home range as small as 10 square kilometers but usually it varies between $80 - 500$ square kilometers.

Lynx are mainly active after sunset and rest during the day time. It is observed that distances covered during night time vary from $1 - 45$ kilometers while males travel more during the mating season. On the other hand females with kittens move very short distances and stay in the proximity of a kill for several days. Lynx walk at a steady pace but during hunting they can leap as long as $6 - 8$ meters. A Lynx foot print resembles with that of a cat but it is usually larger. The thick fur around the toes of a lynx makes rounded circles in snow. Figure 3.3 shows a lynx[3] and the foot print; the foot size is $7 - 9$cm in length and $6 - 12$cm in width.

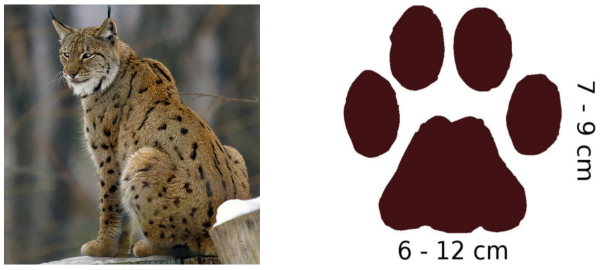

Figure 3.3: Lynx and foot size

Wolverine

A female wolverine can usually have a litter of $2 - 3$ cubs and occasionally 1 or 5 can be born. The cubs start walking with the mother at $9 - 10$ weeks. The mating season is from June to August while birth is in January to March. The wolverine is generally a solitary animal but the social behavior and dispersal is inadequately recorded. Usually the home range of a male can vary from $100 - 500$ square kilometers while that of a female can be $100 - 200$ square kilometers (Landa et al., 2000).

---

[3] http://creativecommons.org/licenses/by-sa/2.0/de/deed.en

Wolverines are generally scavengers that feed on remains left by other predators but can also hunt domestic sheep and semi domestic reindeer. Wolverines usually run or leap and leave tracks in pairs of two and three. The foot size of a wolverine is unexpectedly large and enables them to move around easily and rapidly in snow. The foot print is easily distinguished from other animals. Figure 3.4 shows a wolverine[4] and the foot print; the length is $8 - 10$cm while the width is $6 - 14$cm.

Figure 3.4: Wolverine and foot size

3.2 Data Format

The procedure used for the collection of data involves multiple observers spread over a random space in time. This results in a dataset that contains multiple observations or measurements from a single animal received during various times of the year. A single observation in the dataset mainly includes the geographical position of an animal in the standard YKJ co-ordinate system, the time and date of observation, the foot print width and length which is measured in centimeters, and the number of animals in the family or a pack(in case of wolves). Furthermore, additional fields of the data comprise of the game management district information, the type of species observed and some notes for individual special cases as reported by the volunteer.

The dataset can be represented as a structure as shown in table 3.1. If the total number of observations are T then each feature of the data is stored as an array of size $1 \times T$. The data set is a $N \times T$ structure where N is the total number of observations. The analysis on this data is performed separately for each animal type for example, a single analysis performed using the algorithm would only compute the total number of bears. This is because associating observations from different

---

[4] By Jeffrey C. Lewis [Public domain], via Wikimedia Commons. http://creativecommons.org/licenses/by-sa/3.0/

animals is incorrect. The large carnivores have the Finnish names: karhu(bear), susi(wolf), ilves(lynx) and ahma(wolverine).

No.	Field Type	Array Size
1.	Observation-ID	$1 \times T$ of T
2.	Communication source	$1 \times T$ of T
3.	Game management district	$1 \times T$ of T
4.	Observation period	$1 \times T$ of T
5.	Observation date	$1 \times T$ of T
6.	Species type	$1 \times T$ of T
7.	Observation time	$1 \times T$ of T
8.	Number of adults	$1 \times T$ of T
9.	Number of cubs	$1 \times T$ of T
10.	Number of 1-year old	$1 \times T$ of T
11.	Observation type	$1 \times T$ of T
12.	1^{st} foot print width	$1 \times T$ of T
13.	1^{st} foot print length	$1 \times T$ of T
14.	2^{nd} foot print width	$1 \times T$ of T
15.	2^{nd} foot print length	$1 \times T$ of T
16.	3^{rd} foot print width	$1 \times T$ of T
17.	3^{rd} foot print length	$1 \times T$ of T
18.	Distance of nearest house	$1 \times T$ of T
19.	Target contact person	$1 \times T$ of T
20.	Case based notes	$1 \times T$ of T
21.	YKJ Co-ordinate - X	$1 \times T$ of T
22.	YKJ Co-ordinate - Y	$1 \times T$ of T

Table 3.1: Data Attributes

The tables 3.2 to 3.5 show some statistics about the observations where the columns represent the following information.

- A - Total observations.
- B - Total foot measurements.
- C - Observations with at least 1 adult and 1 cub.
- D - Observations with at least 1 adult, 1 cub and 1 foot measurement.

Table 3.2 shows bear sampling statistics; the number of observations have become two fold in the year 2009 as compared to 2001. In the year 2009 a total of 8020 observations were recorded. However, it was observed that from the start of April to the end of September 6918 samples were collected while only 1102 were collected from October to March. This can be explained by the fact that bears hibernate during the winter time. The number of samples with at least a single adult and a single cub are very low as compared to the total number of observations. Similar pattern is observed when at least a single foot measurement is included in to the conditions.

Tables 3.3, 3.4 and 3.5 show that the sampling effort in case of wolf, lynx and wolverine has gradually increased during the 9 years. Analysis of 2009 data of these three animals showed that a very high number of observations were collected during autumn and winter (October to March) while fewer observations were made during spring and summer (April to September). The number of foot size measurements recorded is very low in the data as compared to the total number of observations.

Year	A	B	C	D
2001	4808	3494	317	210
2002	4808	3250	270	184
2003	4228	2930	268	149
2004	4625	3432	348	223
2005	5631	3314	393	220
2006	5247	3872	403	221
2007	6147	4468	457	276
2008	7023	5347	542	326
2009	8020	6181	731	433

Table 3.2: Bear Observations

Year	A	B	C	D
2001	2015	821	66	54
2002	2497	1018	74	59
2003	2526	1240	122	82
2004	4304	2021	194	151
2005	4780	1745	288	199
2006	4790	1993	239	193
2007	5725	2546	187	140
2008	5358	2845	188	130
2009	4742	2266	135	72

Table 3.3: Wolf Observations

Year	A	B	C	D
2001	4490	1978	457	378
2002	5691	2586	640	519
2003	6934	3364	936	735
2004	9484	4774	1195	923
2005	11805	4891	1480	833
2006	13613	7418	1875	1365
2007	12064	5872	1803	1376
2008	19030	9571	2945	2132
2009	22682	12727	3577	2274

Table 3.4: Lynx Observations

Year	A	B	C	D
2001	540	219	5	4
2002	804	265	8	6
2003	815	270	5	5
2004	882	320	5	3
2005	1024	295	12	7
2006	915	301	16	15
2007	859	243	9	3
2008	1530	557	9	8
2009	1053	410	9	8

Table 3.5: Wolverine Observations

3.3 Model

We have used the state-space model framework as the basis for representing the dynamic and measurement models. The dynamic animal movement models given as linear stochastic differential equations (SDE) can be discretized in order to solve the filtering problem. The discretization of linear SDE results in a discrete-time linear Gaussian model, which is suitable for the Kalman filter. We can write a linear (time-invariant) SDE in white noise notation as (Øksendal, 2003; Grewal et al., 2001; Särkkä, 2006)

$$\frac{d\boldsymbol{x}(t)}{dt} = \boldsymbol{F}\,\boldsymbol{x}(t) + \boldsymbol{L}\,\boldsymbol{w}(t)\ , \tag{3.1}$$

where $\boldsymbol{x}(t)$ is a $n-$dimensional state vector at time t, $\boldsymbol{F}$ is a $n \times n$ constant coefficient matrix, $\boldsymbol{w}(t)$ is a Gaussian white noise process with a spectral density matrix $\boldsymbol{Q}_c$ and $\boldsymbol{L}$ is a constant matrix.

Solution of linear SDE

We solve the linear stochastic differential equation given in Equation (3.1) by premultiplying the integrating factor $e^{\boldsymbol{F}t}$ in matrix exponential form as

$$\begin{aligned} e^{-\boldsymbol{F}t}\Big(\frac{d\boldsymbol{x}(t)}{dt} - \boldsymbol{F}\,\boldsymbol{x}(t)\Big) &= e^{-\boldsymbol{F}t}\Big(\boldsymbol{L}\,w(t)\Big) \\ \Longrightarrow\ \frac{d}{dt}\Big(e^{-\boldsymbol{F}t}\,\boldsymbol{x}(t)\Big) &= e^{-\boldsymbol{F}t}\Big(\boldsymbol{L}\,w(t)\Big)\ , \end{aligned}$$

integrating the above expression between t_0 and t

$$\begin{aligned} \int_{t_0}^{t} \frac{d}{dt}\Big(e^{-\boldsymbol{F}\tau}\,\boldsymbol{x}(\tau)\Big) &= \int_{t_0}^{t} e^{-\boldsymbol{F}\tau}\,\boldsymbol{L}\,w(\tau)\,d\tau \\ \Longrightarrow\ \boldsymbol{x}(t) = e^{\boldsymbol{F}(t-t_0)}\,\boldsymbol{x}(t_0) &+ \int_{t_0}^{t} e^{\boldsymbol{F}(t-\tau)}\,\boldsymbol{L}\,w(\tau)\,d\tau\ . \end{aligned} \tag{3.2}$$

The mean and covariance can be computed from Equation (3.2). The solution to the linear SDE is a Gaussian process with mean and covariance (Grewal et al., 2001)

$$\boldsymbol{m}(t) = \exp(\boldsymbol{F}(t-t_0))\,\boldsymbol{x}(t_0) \tag{3.3}$$

$$\begin{aligned} \boldsymbol{P}(t) &= \exp(\boldsymbol{F}(t-t_0))\,\boldsymbol{P}(t_0)\,\exp(\boldsymbol{F}(t-t_0))^T \\ &\quad + \int_{t_0}^{t} \exp(\boldsymbol{F}(t-t_0))\,\boldsymbol{L}\,\boldsymbol{Q}_c\,\boldsymbol{L}^T\,\exp(\boldsymbol{F}(t-t_0))^T\,dt_0\ , \end{aligned} \tag{3.4}$$

where $\boldsymbol{x}(t_0) \sim \mathrm{N}(\boldsymbol{m}(t_0), \boldsymbol{P}(t_0))$ and exp(.) is the matrix exponential function.

Discretization

Because t_0 in Equations (3.3) and (3.4) is arbitrary, we can also express the solution in recursive form as follows:

$$\boldsymbol{m}(t_k) = \underbrace{\exp(\boldsymbol{F}(t_k - t_{k-1}))}_{\boldsymbol{A}_{k-1}} \boldsymbol{m}(t_{k-1}) \tag{3.5}$$

$$\begin{aligned}\boldsymbol{P}(t_k) = & \underbrace{\exp(\boldsymbol{F}(t_k - t_{k-1}))}_{\boldsymbol{A}_{k-1}} \boldsymbol{P}(t_{k-1}) \underbrace{\exp(\boldsymbol{F}(t_k - t_{k-1}))^T}_{\boldsymbol{A}_{k-1}^T} \\ & + \underbrace{\int_{t_{k-1}}^{t_k} \exp(\boldsymbol{F}(t_k - t_{k-1}))\, \boldsymbol{L}\, \boldsymbol{Q}_c\, \boldsymbol{L}^T \exp(\boldsymbol{F}(t_k - t_{k-1}))^T \, dt_{k-1}}_{\boldsymbol{Q}_{k-1}} \,,\end{aligned} \tag{3.6}$$

where $\boldsymbol{x}(t_{k-1}) \sim \mathrm{N}(\boldsymbol{m}(t_{k-1}), \boldsymbol{P}(t_{k-1}))$ and exp(.) is the matrix exponential function. Thus the mean and covariance of the solution in Equations (3.3) and (3.4) at discrete instances $t_1, t_2, \ldots$ are given by the recursive equations;

$$\mathbf{m}_k = \mathbf{A}_{k-1}\mathbf{m}_{k-1} \tag{3.7}$$

$$\mathbf{P}_k = \mathbf{A}_{k-1}\mathbf{P}_{k-1}\mathbf{A}_{k-1}^T + \mathbf{Q}_{k-1} \,, \tag{3.8}$$

where $\boldsymbol{m}_k = \boldsymbol{m}(t_k)$ and $\boldsymbol{P}_k = \boldsymbol{P}(t_k)$. By comparing to Algorithm 2.3.1, we can see that this is exactly the Kalman filter prediction step.

3.4 Method

We have used the Rao-Blackwellized Monte Carlo data association (RBMCDA) algorithm, designed to solve the problem of data association in case of both ‘a known number of targets’ and ‘an unknown number of targets’, presented in (Särkkä et al., 2007). The idea of Rao-Blackwellization is implemented in such a way that the individual states of the targets is estimated analytically, for example, Kalman filter is used when the dynamic and measurement models are linear Gaussian. State estimation is conditional on the data associations, which are sampled using sequential importance resampling (SIR).

RBMCDA with Known Number of Targets

Consider the state-space model given as

$$\begin{aligned}\boldsymbol{x}_{j,k} &= \boldsymbol{A}_{j,k-1}\boldsymbol{x}_{j,k-1} + \boldsymbol{q}_{j,k-1} \\ \boldsymbol{y}_k &= \boldsymbol{H}_{j,k}\boldsymbol{x}_{j,k} + \boldsymbol{r}_{j,k}\end{aligned} \tag{3.9}$$

where number of targets $j = 1, \dots, T$ and the process noise $\boldsymbol{q}_{j,k-1}$ and measurement noise $\boldsymbol{r}_{j,k}$ terms are zero mean with covariance matrices $\boldsymbol{Q}_{j,k-1}$ and $\boldsymbol{R}_{j,k}$, respectively.

$$\begin{aligned} \boldsymbol{q}_{j,k-1} &\sim \mathrm{N}(0, \boldsymbol{Q}_{j,k-1}) \\ \boldsymbol{r}_{j,k} &\sim \mathrm{N}(0, \boldsymbol{R}_{j,k}) \ . \end{aligned} \tag{3.10}$$

The problem is to estimate the states of T targets from noisy and cluttered measurements $\boldsymbol{y}_{1:k}$. This is possible only if the sources of the measurements can be distinguished, that is, which measurement has originated from which target. The measurements can also be 'clutter measurements'. Clutter or false alarm refers to the measurements that originate from some other source than from the targets that we are tracking. Therefore, a single measurement at time step k can originate from one of two different sources; one of the known targets $j = 1, \dots, T$ or clutter $j = 0$.

The RBMCDA algorithm basically involves the same steps as already described in the Algorithm 2.3.3. Because the latent variable is discrete, we can use the optimal importance distribution in the Rao-Blackwellized particle filter for solving the data association problem. The clutter is assumed to be uniformly distributed on the observation area with volume V and thus the probability density of a cluttered measurement $\boldsymbol{y}_k$ is given as

$$p(\boldsymbol{y}_k | c_k = 0) = 1/V, \tag{3.11}$$

where c_k is the data association indicator or latent variable as in the case of the conditionally Gaussian Markov models. The data association indicator has the value $c_k = j$ for targets $j = 1, \dots, T$ and the probability of the measurement originated from a target is same as the Kalman filter likelihood given by

$$p(\boldsymbol{y}_k | \boldsymbol{x}_{j,k}, c_k = j) = \mathrm{N}(\boldsymbol{y}_k | \boldsymbol{H}_{j,k} \boldsymbol{x}_{j,k}, \boldsymbol{R}_{j,k}) \ , \tag{3.12}$$

where the measurement model matrices $\boldsymbol{H}_{j,k}$ and $\boldsymbol{R}_{j,k}$ can be different for each target. The target and clutter association priors are assumed to be known and given by $p(c_k | c_{1:k-1})$, for example, when there are only 2 targets and the clutter density is 50% the prior probabilities would be

$$\begin{aligned} p(c_k = 0) &= 0.5 \\ p(c_k = 1) &= 0.25 \\ p(c_k = 2) &= 0.25 \ . \end{aligned} \tag{3.13}$$

The optimal distribution required for the SIR can now be written as $p(c_k | \boldsymbol{y}_{1:k}, c_{1:k-1})$.

For the implementation of RBMCDA algorithm with N number of particles, the algorithm state stores and updates

$$\begin{aligned}
&\text{particle 1}: \{c^{(1)}_{1,k}, \boldsymbol{m}^{(1)}_{1,k}, \boldsymbol{P}^{(1)}_{1,k}, c^{(1)}_{2,k}, \boldsymbol{m}^{(1)}_{2,k}, \boldsymbol{P}^{(1)}_{2,k}, \ldots, c^{(1)}_{T,k}, \boldsymbol{m}^{(1)}_{T,k}, \boldsymbol{P}^{(1)}_{T,k}, w^{(1)}_k\} \\
&\text{particle 2}: \{c^{(2)}_{1,k}, \boldsymbol{m}^{(2)}_{1,k}, \boldsymbol{P}^{(2)}_{1,k}, c^{(2)}_{2,k}, \boldsymbol{m}^{(2)}_{2,k}, \boldsymbol{P}^{(2)}_{2,k}, \ldots, c^{(2)}_{T,k}, \boldsymbol{m}^{(2)}_{T,k}, \boldsymbol{P}^{(2)}_{T,k}, w^{(2)}_k\} \\
&\qquad\qquad \vdots \\
&\text{particle N}: \{c^{(N)}_{1,k}, \boldsymbol{m}^{(N)}_{1,k}, \boldsymbol{P}^{(N)}_{1,k}, c^{(N)}_{2,k}, \boldsymbol{m}^{(N)}_{2,k}, \boldsymbol{P}^{(N)}_{2,k}, \ldots, c^{(N)}_{T,k}, \boldsymbol{m}^{(N)}_{T,k}, \boldsymbol{P}^{(N)}_{T,k}, w^{(N)}_k\}\ ,
\end{aligned}$$

where $c^{(i)}_{1:T,k}$ are the data association indicators for the targets which can have integer values $0, \ldots, T$, and $\boldsymbol{m}^{(i)}_{1:T,k}, \boldsymbol{P}^{(i)}_{1:T,k}$ are the means and covariances of the targets and $w^{(i)}_k$ is the importance weight of each particle $i = 1, \ldots, N$.

The optimal importance distributions for N particles are $p(c_k|\boldsymbol{y}_{1:k}, c^{(i)}_{1:k-1})$, where $i = 1, \ldots, N$. The following steps have to be performed in order to sample from the optimal distribution at each step k,

1. Compute the clutter association probability as

$$\hat{\pi}^{(i)}_0 = p(\boldsymbol{y}_k|c^{(i)}_k = 0, \boldsymbol{y}_{1:k-1}, c^{(i)}_{1:k-1})p(c^{(i)}_k = 0)$$

2. Compute the target association probability for each target $j = 1, \ldots, T$ as

$$\hat{\pi}^{(i)}_j = p(\boldsymbol{y}_k|c^{(i)}_k = j, \boldsymbol{y}_{1:k-1}, c^{(i)}_{1:k-1})p(c^{(i)}_k = j)$$

3. Normalize the importance distribution as

$$\pi^{(i)}_j = \frac{\hat{\pi}^{(i)}_j}{\sum_{t=0}^{T} \hat{\pi}^{(i)}_t}, \qquad j = 0, \ldots, T$$

4. Sample new associations to targets and clutter as
    - Draw $c^{(i)}_k = 0$ with probability $\pi^{(i)}_0$
    - Draw $c^{(i)}_k = 1$ with probability $\pi^{(i)}_1$
    - ...
    - Draw $c^{(i)}_k = T$ with probability $\pi^{(i)}_T$.

RBMCDA with Unknown Number of Targets

Again the aim is to estimate the state of the targets and the same model can be considered as given in Equation (3.9). However, it is assumed that a very large and constant number of targets T_∞ are always available to be detected but only a varying number of them are visible or alive. Therefore, a single measurement at time step k can be assumed to be originated from one of three different sources;

- one of the existing targets $j = 1, \ldots, T$.
- a new target $j = T + 1$.
- clutter $j = 0$.

The probability density of a cluttered measurement is the same as in Equation (3.11) and the the probability of a measurement originated from an existing target is the same as in Equation (3.12). However, the probability of a measurement originated from a new target would be the Kalman filter likelihood which can be computed given the initial mean $\boldsymbol{m}_0$ and initial process noise covariance $\boldsymbol{P}_0$, using the measurement likelihood

$$p(\boldsymbol{y}_k|\boldsymbol{x}_0, c_k = j) = \mathrm{N}(\boldsymbol{y}_k|\boldsymbol{H}_{j=T+1,k}\boldsymbol{x}_0, \boldsymbol{R}_{j=T+1,k}) \ , \tag{3.14}$$

where c_k is the data association indicator which has a value $j = T + 1$ and the measurement model matrices $\boldsymbol{H}_{j=T+1,k}$ and $\boldsymbol{R}_{j=T+1,k}$ can be different for the new target. The association of a measurement to a new target is called a birth. The target and clutter associations probabilities can be modeled as

$$p(b_k, c_k|c_{1:k-1}) = \begin{cases} p_b & ,\text{event}(1) \\ (1 - p_b)p(c_k|c_{1:k-1}) & ,\text{event}(2) \\ 0 & ,\text{event}(3) \end{cases} \tag{3.15}$$

where event(1) indicates the birth of a new target which has a probability p_b, event(2) indicates the probabilities of association to an existing target or clutter and all other events have zero probability. Each target has a life time t_d after getting associated to a measurement. The time to death probability density is given by

$$t_d \sim p(t_d), \tag{3.16}$$

which can be, for example, an exponential or gamma distribution.

Similar steps can be followed for the implementation of RBMCDA with ‘an unknown number of targets’ as in the case of ‘a known number of targets’. The algorithm state stores and updates

$$\begin{aligned}
&\text{particle 1}: \{\boldsymbol{e}_k^{(1)}, c_{1,k}^{(1)}, \boldsymbol{m}_{1,k}^{(1)}, \boldsymbol{P}_{1,k}^{(1)}, c_{2,k}^{(1)}, \boldsymbol{m}_{2,k}^{(1)}, \boldsymbol{P}_{2,k}^{(1)}, \ldots, c_{T_\infty,k}^{(1)}, \boldsymbol{m}_{T_\infty,k}^{(1)}, \boldsymbol{P}_{T_\infty,k}^{(1)}, w_k^{(1)}\} \\
&\text{particle 2}: \{\boldsymbol{e}_k^{(2)}, c_{1,k}^{(2)}, \boldsymbol{m}_{1,k}^{(2)}, \boldsymbol{P}_{1,k}^{(2)}, c_{2,k}^{(2)}, \boldsymbol{m}_{2,k}^{(2)}, \boldsymbol{P}_{2,k}^{(2)}, \ldots, c_{T_\infty,k}^{(2)}, \boldsymbol{m}_{T_\infty,k}^{(2)}, \boldsymbol{P}_{T_\infty,k}^{(2)}, w_k^{(2)}\} \\
&\qquad\qquad\vdots \\
&\text{particle N}: \{\boldsymbol{e}_k^{(N)}, c_{1,k}^{(N)}, \boldsymbol{m}_{1,k}^{(N)}, \boldsymbol{P}_{1,k}^{(N)}, c_{2,k}^{(N)}, \boldsymbol{m}_{2,k}^{(N)}, \boldsymbol{P}_{2,k}^{(N)}, \ldots, c_{T_\infty,k}^{(N)}, \boldsymbol{m}_{T_\infty,k}^{(N)}\boldsymbol{P}_{T_\infty,k}^{(N)}, w_k^{(N)}\} \ ,
\end{aligned}$$

where $\boldsymbol{e}_k^{(i)}$ is the life indicator vector of length $T_k^{(i)}$, $c_{1:T,k}^{(i)}$ are the data association indicators for the targets which can have integer values $0, \ldots, T_k^{(i)}$, and $\boldsymbol{m}_{1:T,k}^{(i)}, \boldsymbol{P}_{1:T,k}^{(i)}$ are the means and covariances of the targets and $w_k^{(i)}$ is the importance weight of each particle $i = 1, \ldots, N$. The number of targets $\hat{T}_k^{(i)}$ in each particle $i = 1, \ldots, N$ at time step k can be different and the expected number of targets at time step k can be computed by a weighted sum over the particles as

$$T_k = \sum_{i=1}^{N} w_k^{(i)} \; \hat{T}_k^{(i)} \; . \tag{3.17}$$

Chapter 4

Results

In this chapter, we present the results of applying RBMCDA to the animal observation datasets. We mainly present application of a static model and a dynamic model for the estimation of bear population in the year 2010. We also numerically show the estimated population size of bear, wolf, lynx and wolverine for the year 2009. The results section provides with an adequate explanation of the models used in the analysis of the 2010 dataset. Therefore, similar procedures could be applied to any other dataset from the year 2001 to 2008.

In the manual counting method, the *Finnish Game and Fisheries Research Institute* considers observations with at least one adult and one cub as being the most reliable for population estimation of the animals. Therefore, we have also used similar observations from the datasets in order to obtain comparable final results. We use the YKJ coordinates as measurements of the kinematic part of the state and the foot widths are the attribute measurements in the analysis. For the analysis of bear datasets a single foot width indicates the age of a bear hence adult bears and cubs can be distinguished based on this information. However, some foot measurements have to be categorized depending on the time of observation. The Table[1] 4.1 shows the foot width sizes for adults and cubs during different seasons of the year. The one year olds (cubs from previous year) are also treated as cubs in our analysis.

Season	Cub	1 year old	Adult
Spring	3.5 – 5 (cm)	4 – 7 (cm)	6 – 9 (cm)
Summer	6 – 9 (cm)	7 – 10 (cm)	8 – 11 (cm)
Autumn	> 9 (cm)	> 10 (cm)	> 11 (cm)

Table 4.1: Bear foot widths for different seasons

---

[1] courtesy Finnish Game and Fisheries Research Institute.

Process Model

The process model is basically a zero drift random walk model that can be written in continuous form as

$$\begin{aligned}\frac{dx}{dt} &= w_1\\ \frac{dy}{dt} &= w_2\\ \frac{df^1}{dt} &= w_3\\ \frac{df^2}{dt} &= w_4\\ \vdots &= \vdots\\ \frac{df^M}{dt} &= w_M \ ,\end{aligned} \tag{4.1}$$

where x and y are the coordinates, and $f^1, \ldots, f^M$ are foot widths, and $w_1 \ldots, w_M$ are Gaussian white noise processes with a diagonal spectral density matrix $\boldsymbol{Q}_c$. The discretized model can be written as

$$\underbrace{\begin{pmatrix} x_{j,k} \\ y_{j,k} \\ f^1_{j,k} \\ f^2_{j,k} \\ \vdots \\ f^M_{j,k} \end{pmatrix}}_{\boldsymbol{x}_{j,k}} = \underbrace{\begin{pmatrix} 1 & 0 & 0 & 0 & \ldots & 0 \\ 0 & 1 & 0 & 0 & \ldots & 0 \\ 0 & 0 & 1 & 0 & \ldots & 0 \\ 0 & 0 & 0 & 1 & . & 0 \\ \vdots & \vdots & \vdots & . & \ddots & . \\ 0 & 0 & 0 & 0 & 0 & 1 \end{pmatrix}}_{\boldsymbol{A}_{j,k-1}} \underbrace{\begin{pmatrix} x_{j,k-1} \\ y_{j,k-1} \\ f^1_{j,k-1} \\ f^2_{j,k-1} \\ \vdots \\ f^M_{j,k-1} \end{pmatrix}}_{\boldsymbol{x}_{j,k-1}} + \boldsymbol{q}_{k-1} \ , \tag{4.2}$$

where the state vector $\boldsymbol{x}_{j,k}$ consists of the position $(x_{j,k}, y_{j,k})$ of the target j and the foot width measurements $f^m_{j,k} : \ m = 1, \ldots, M$. $\boldsymbol{A}_{j,k-1}$ is the transition matrix of size $(M + 2 \times M + 2)$ and $\boldsymbol{q}_{k-1} \sim \mathrm{N}(0, \boldsymbol{Q})$ is the zero mean Gaussian process noise with covariance matrix

$$\boldsymbol{Q} = \begin{pmatrix} q_x\Delta t & 0 & 0 & \ldots & 0 \\ 0 & q_y\Delta t & 0 & \ldots & 0 \\ 0 & 0 & q^1_f\Delta t & . & 0 \\ \vdots & \vdots & . & \ddots & . \\ 0 & 0 & 0 & 0 & q^M_f\Delta t \end{pmatrix} . \tag{4.3}$$

Measurement Model

The number of foot measurements obtained can vary in different observations because a single observation can include different number of animals. On the other hand, there can be observations without any foot width measurements due to sighting based data. Assuming there can be $m = 0, \dots, M$ number of foot width measurements $f_{j,k}^{m}$ in a single observation then the measurement model matrix is a $(m + 2 \times 2M + 2)$ size matrix. The measurement model in general is of the form given in the Equation (3.9). Furthermore, we have used four different types of measurement model and noise matrices given in a generic form as

- Case 1: Only positional information is available then

  $$\begin{gathered}\boldsymbol{H}_{j,k} = \begin{pmatrix} 1 & 0 & 0 & \dots & 0 \\ 0 & 1 & 0 & \dots & 0 \end{pmatrix}_{m+2 \times 2M+2} \\ \text{and} \\ \boldsymbol{R}_{j,k} = \begin{pmatrix} \sigma_x^2 & 0 \\ 0 & \sigma_y^2 \end{pmatrix}_{m+2 \times m+2}, \end{gathered} \tag{4.4}$$

  where $m = 0$, σ_x^2 and σ_y^2 are observation noise variances.

- Case 2: Only adult foot width measurements are available along with positional information then

  $$\begin{gathered}\boldsymbol{H}_{j,k} = \begin{pmatrix} 1 & 0 & 0 & 0 & \dots & 0 & \dots & 0 \\ 0 & 1 & 0 & 0 & \dots & 0 & \dots & 0 \\ 0 & 0 & 1 & 0 & \dots & 0 & \dots & 0 \\ \vdots & \vdots & . & \ddots & . & \vdots & . & \vdots \\ 0 & 0 & 0 & 0 & 1 & 0 & \dots & 0 \end{pmatrix}_{m+2 \times 2M+2} \\ \text{and} \\ \boldsymbol{R}_{j,k} = \begin{pmatrix} \sigma_x^2 & 0 & 0 & \dots & 0 \\ 0 & \sigma_y^2 & 0 & \dots & 0 \\ 0 & 0 & \sigma_{f_a}^2 & . & 0 \\ \vdots & \vdots & . & \ddots & 0 \\ 0 & 0 & 0 & 0 & \sigma_{f_a}^2 \end{pmatrix}_{m+2 \times m+2}, \end{gathered} \tag{4.5}$$

  where $m = 1, \dots, M$, σ_x^2, σ_y^2 and $\sigma_{f_a}^2$ are observation noise variances.

- Case 3: Only cub foot width measurements are available along with positional information then

$$\begin{gathered}
\boldsymbol{H}_{j,k} = \begin{pmatrix}
1 & 0 & 0 & \dots & 0 & 0 & \dots & 0 \\
0 & 1 & 0 & \dots & 0 & 0 & \dots & 0 \\
0 & 0 & 0 & \dots & 0 & 1 & . & 0 \\
\vdots & \vdots & . & \ddots & . & . & \ddots & . \\
0 & 0 & 0 & 0 & 0 & 0 & 0 & 1
\end{pmatrix}_{m+2 \times 2M+2} \\
\text{and} \\
\boldsymbol{R}_{j,k} = \begin{pmatrix}
\sigma_x^2 & 0 & 0 & \dots & 0 \\
0 & \sigma_y^2 & 0 & \dots & 0 \\
0 & 0 & \sigma_{f_c}^2 & . & 0 \\
\vdots & \vdots & . & \ddots & 0 \\
0 & 0 & 0 & 0 & \sigma_{f_c}^2
\end{pmatrix}_{m+2 \times m+2} ,
\end{gathered} \tag{4.6}$$

where $m = 1, \dots, M$, σ_x^2, σ_y^2 and $\sigma_{f_a}^2$ are observation noise variances.

- Case 4: Both adult and cub foot widths are available along with positional information

$$\begin{gathered}
\boldsymbol{H}_{j,k} = \begin{pmatrix}
1 & 0 & 0 & 0 & \dots & 0 & 0 & \dots & 0 \\
0 & 1 & 0 & 0 & \dots & 0 & 0 & \dots & 0 \\
0 & 0 & 1 & 0 & \dots & 0 & 0 & \dots & 0 \\
\vdots & \vdots & . & \ddots & . & \vdots & \vdots & . & \vdots \\
0 & 0 & 0 & 0 & 1 & 0 & 0 & \dots & 0 \\
0 & 0 & 0 & 0 & 0 & 0 & 1 & . & 0 \\
\vdots & \vdots & \vdots & \vdots & \vdots & \vdots & . & \ddots & . \\
0 & 0 & 0 & 0 & 0 & 0 & 0 & 0 & 1
\end{pmatrix}_{m+2 \times 2M+2} \\
\text{and} \\
\boldsymbol{R}_{j,k} = \begin{pmatrix}
\sigma_x^2 & 0 & 0 & \dots & 0 & 0 & \dots & 0 \\
0 & \sigma_y^2 & 0 & \dots & 0 & 0 & \dots & 0 \\
0 & 0 & \sigma_{f_a}^2 & . & 0 & 0 & \dots & 0 \\
\vdots & \vdots & . & \ddots & 0 & 0 & \dots & 0 \\
0 & 0 & 0 & 0 & \sigma_{f_a}^2 & 0 & \dots & 0 \\
0 & 0 & 0 & 0 & 0 & \sigma_{f_c}^2 & . & \vdots \\
\vdots & \vdots & \vdots & \vdots & \vdots & . & \ddots & 0 \\
0 & 0 & 0 & 0 & 0 & 0 & 0 & \sigma_{f_c}^2
\end{pmatrix}_{m+2 \times m+2} ,
\end{gathered} \tag{4.7}$$

where $m = 1, \dots, M$, σ_x^2, σ_y^2, $\sigma_{f_a}^2$ and $\sigma_{f_c}^2$ are observation noise variances.

A single measurement model matrix and observation noise matrix is selected before the update step of the Rao-Blackwellized Monte Carlo Data Association algorithm. The information in Table 4.1 is used to check whether the foot width measurements belong to adult bears or cubs for the analysis of the bear observations.

Bears 2010

The main reason of illustrating results of bear observations in 2010 with detail is that each observation in this dataset has been labeled with a group number by the researchers at *Finnish Game and Fisheries Research Institute.* Group number refers to an integer value that indicates which observations have originated from the same individuals or family of bears. The highest value of the total group numbers is the the actual number of individuals or families. Subsequently, this value multiplied by a factor of 10 is the total bear population of Finland for a single year. Hence, the results generated by the RBMCDA can also be compared with those of the *Finnish Game and Fisheries Research Institute.*

The dataset consists of a total of 1000 observations where each observation can consist of a single individual or family of bears. The total number of observations with at least a single adult and a single cub is 918. The Figure 4.1 shows two types of observations over the map of Finland: first, observations with at least a single adult and a single cub information and second, all the remaining observations in the dataset. Although, more than 50% of the observations in this dataset consist of foot width measurements only 5% of them have more than 3 foot measurements. Therefore, we choose $M = 3$ foot measurements, hence the state vector is of the form $\boldsymbol{x}_{j,k} = (x_{j,k}\ y_{j,k}\ f^1_{j,k}\ f^2_{j,k}\ f^3_{j,k}\ f^4_{j,k}\ f^5_{j,k}\ f^6_{j,k})^T$.

The number of Monte Carlo samples was 10 in this analysis. This value achieves a reasonable data association approximation and the analysis remains time efficient. We can also use more number of samples but the Kalman filter estimates remain the same due to marginalization and instead of improving the data association approximation, we eventually have more duplicate particles due to sample impoverishment. Hence, the 'total number of targets' remains almost the same but the analysis becomes more time consuming. We use a biased resampling approach and resampling is performed after every 10 steps. This is again a reasonable value in order to avoid degeneracy in the particles.

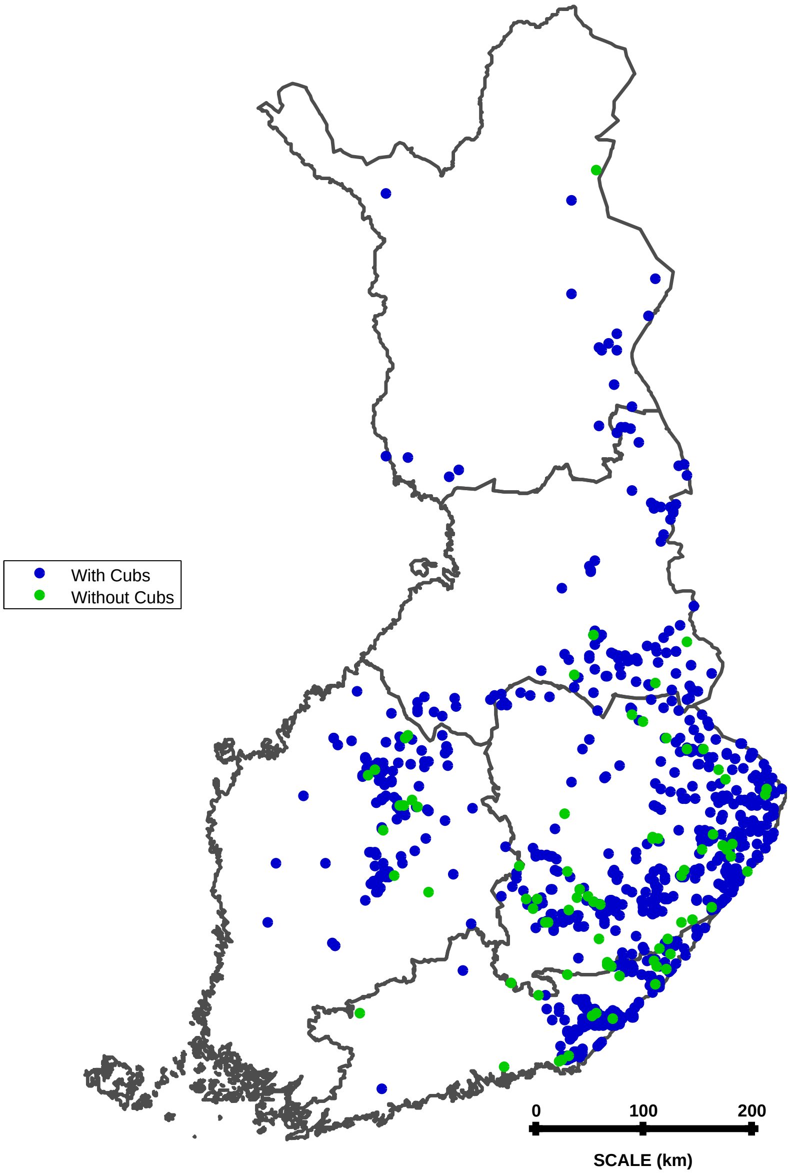

Figure 4.1: Bear observations in Finland for the year 2010. A single observation can consist of a single individual or a family of bears. In this dataset, a large number of observations consist of at least a single adult and a single cub information.

Static Model

For the first case, we assume that the targets are static, that is, the process noise variance in the coordinates is $q_x = 0$ and $q_y = 0$. The process noise variance in the adult foot width size is $q_f^m = 0$. This is because the adult foot width should not change during the year. The process noise variance in cub foot width size is $q_f^m = 1 \times 10^{-6}$, which means that the cub foot width can slightly grow during the year. The time step Δt is irregular depending upon the observation dates and the time unit is days. The clutter density and clutter prior values were 1×10^{-9}, small values were chosen because the measurements did not contain any natural clutter. The prior birth probability was constant $p_b = 1/100$ and deaths do not occur since the targets are always assumed to remain visible after detection.

Each new target has initial mean $\boldsymbol{m}_0 = (0\ 0\ 12\ 12\ 12\ 7\ 7\ 7)^T$ where the first two components represent the mean values of the coordinates, components 3 to 5 represent the mean values of the adult foot widths and the components 6 to 8 represent the mean values of the cub foot widths. The initial covariance matrix is

$$\boldsymbol{P}_0 = \begin{pmatrix} 4 \times 10^{12} & 0 & 0 & 0 & 0 & 0 & 0 & 0 \\ 0 & 4 \times 10^{12} & 0 & 0 & 0 & 0 & 0 & 0 \\ 0 & 0 & 25 & 0 & 0 & 0 & 0 & 0 \\ 0 & 0 & 0 & 25 & 0 & 0 & 0 & 0 \\ 0 & 0 & 0 & 0 & 25 & 0 & 0 & 0 \\ 0 & 0 & 0 & 0 & 0 & 25 & 0 & 0 \\ 0 & 0 & 0 & 0 & 0 & 0 & 25 & 0 \\ 0 & 0 & 0 & 0 & 0 & 0 & 0 & 25 \end{pmatrix}, \tag{4.8}$$

where the first two components of the diagonal represent variances in the coordinates and the components 3 to 8 represent the variances in the foot widths.

The observation noise covariance matrix values were $\sigma_{f_a} = 1$ cm, $\sigma_{f_c} = 1$ cm. These values correspond to the error in measuring the foot widths during surveys. The estimation was performed multiple times with different values of σ_x and σ_y, that is, values between 100 meters to 5000 meters. These values originally correspond to the radial distances of 1 km to 5 km from the observation. The radial distance considered in the manual analysis performed by the Finnish Game and Fisheries Institute is 2 km. We have performed the analysis around this value in order to find the best estimate of the total number of targets.

The Figure 4.2(a) shows that the number of targets increase with increase in observations for all the values of σ_x and σ_y. The best estimate of the total number

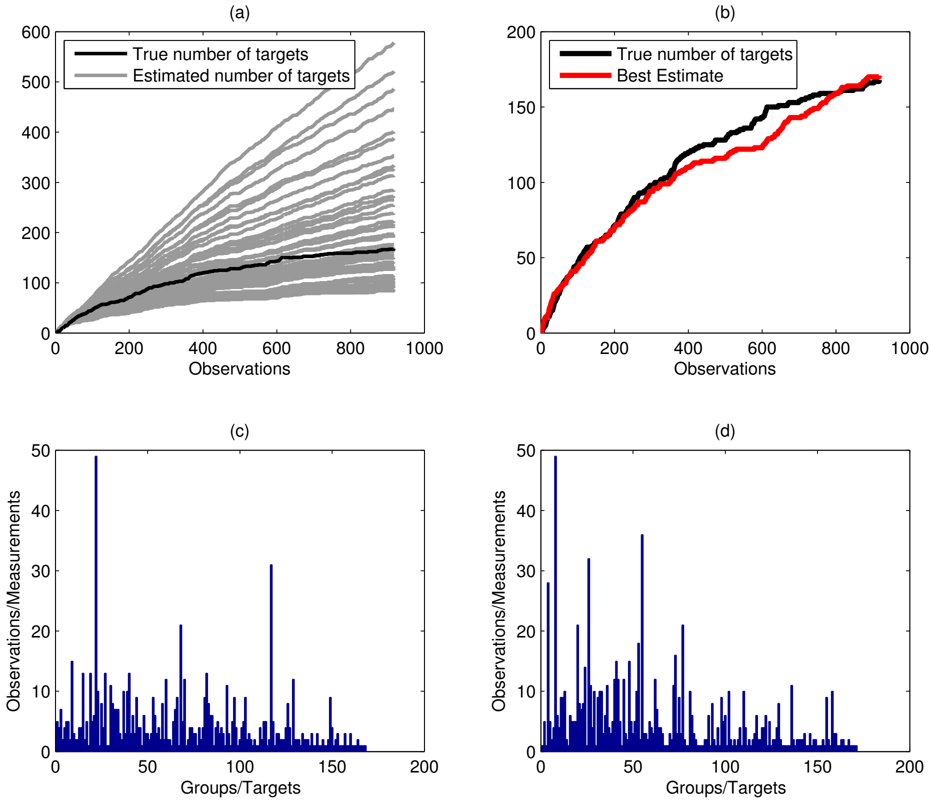

Figure 4.2: (a) Different estimated number of targets in time, (b) Best estimate of the total number of targets, (c) True Group distribution, (d) Group distribution for the best estimate of the total number of targets.

of targets was found with $\sigma_x = 2400$ meters and $\sigma_y = 2400$ meters shown in Figure 4.2(b). The Figure 4.2(c) shows the true distribution of groups while Figure 4.2(d) shows the estimated group distribution of the best estimate. The groups in the estimated group distribution have slightly higher number of observations as compared to the true groups because many observations in the dataset were unlabeled. The results of the data association can also be visualized on the map of Finland as shown in Figure 4.3. It is observed that the true groups are more overlapping as compared to the estimated groups which have more discrete boundaries. Three different examples are illustrated in the Figure 4.4, where (a), (c) and (e) show the true groups at three different locations in Finland, and (b), (d), (f) show the corresponding data associations obtained by RBMCDA.

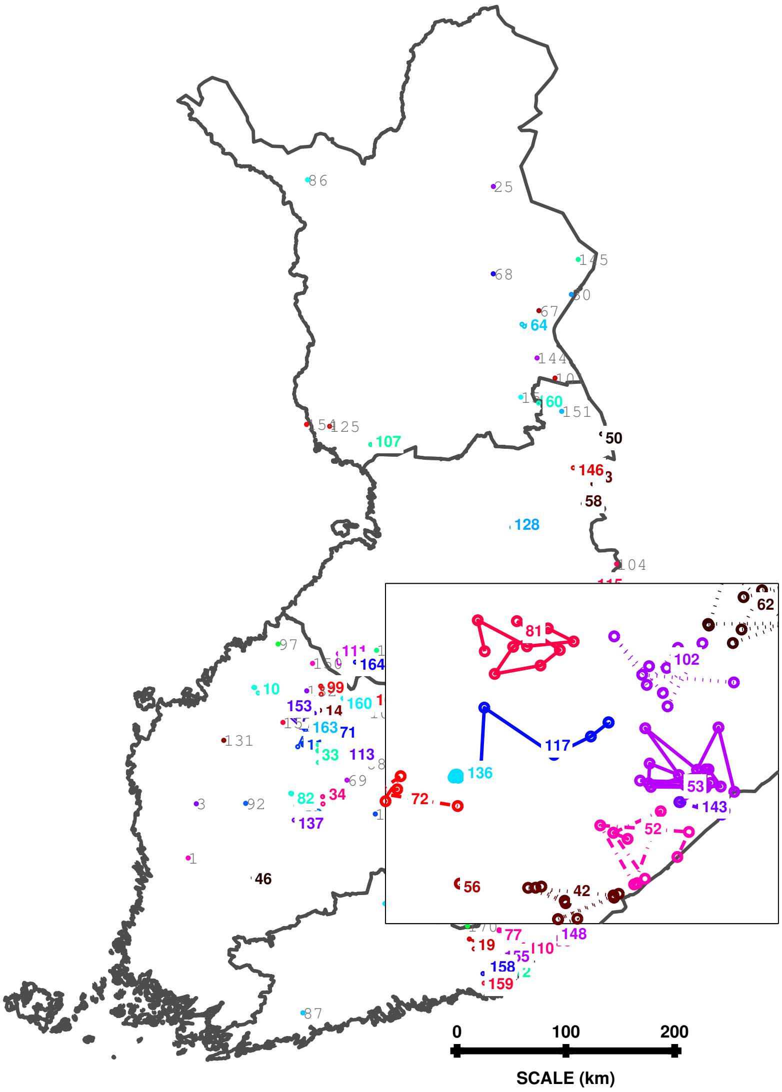

Figure 4.3: The results of the RBMCDA are visualized over the map of Finland. The square box represents a single location close to the southeastern border of Finland. The integer values are group numbers where each group can consist of a single observation or multiple observations.

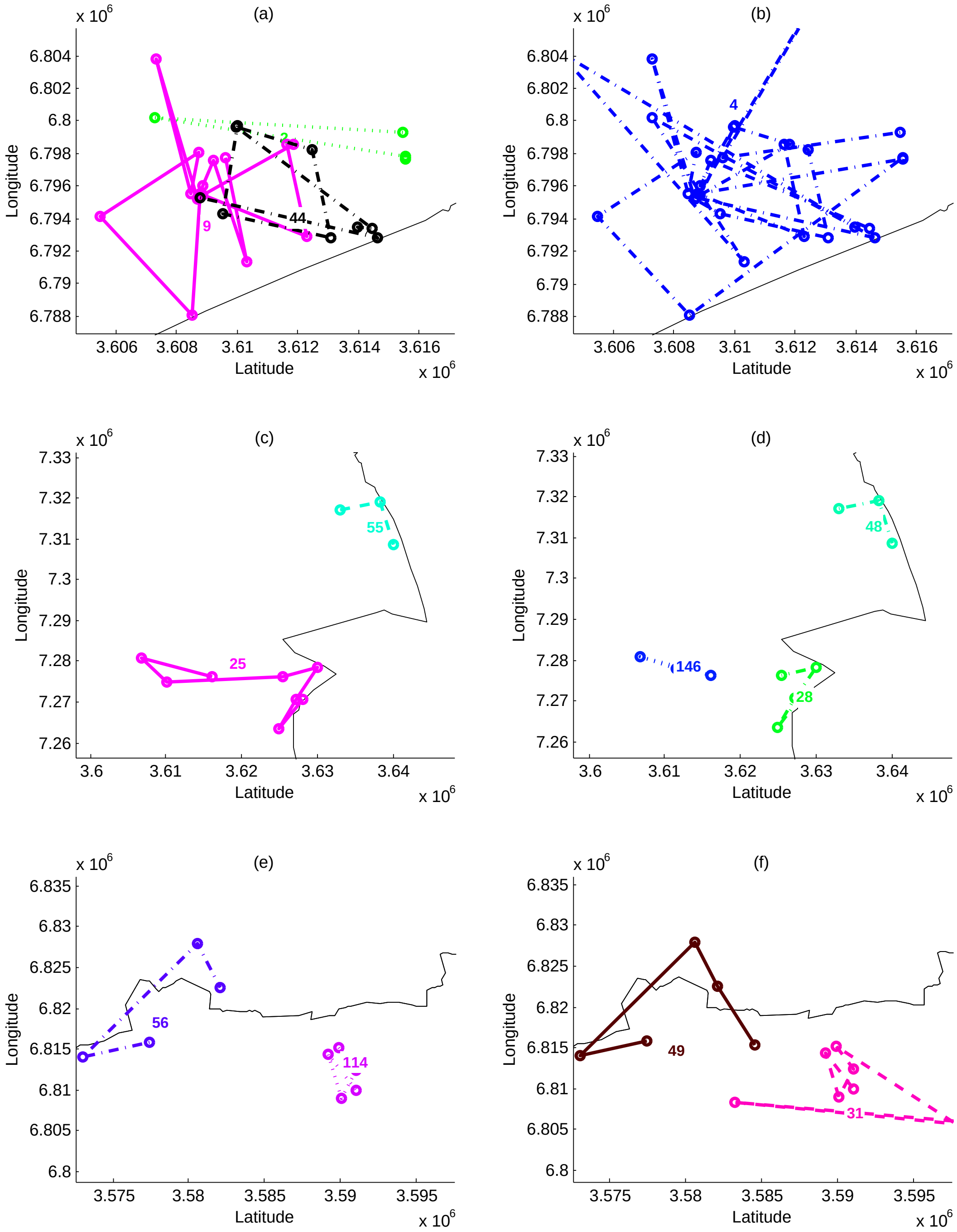

Figure 4.4: Left column: true bear observation groups in three different locations. Right column: corresponding data association results

Dynamic Model

For the second case, we assume that each target exhibits a random walk. The estimation was performed multiple times with different values of q_x and q_y, that is, process noise variance of 100^2 to 2500^2. The observation noise covariance values were $\sigma_x = 0.1$ and $\sigma_y = 0.1$ which corresponds to the observation error in the coordinates. The other parameters in the model were same as given for the static model. The best estimate of the total number of targets was found with $q_x = 1050^2$ and $q_y = 1050^2$ as shown in Figure 4.5(b). The Figure 4.5(c) shows the true distribution of groups while Figure 4.5(d) shows the estimated group distribution of the best estimate. The groups in the estimated group distribution mostly have similar number of observations as compared to the true groups, however, some larger groups have less observations. The comparison of the groups is shown in Figure 4.6, it is observed that the overlapping structure in the true groups is captured in the estimated groups to some extent but there are some incorrect associations as well.

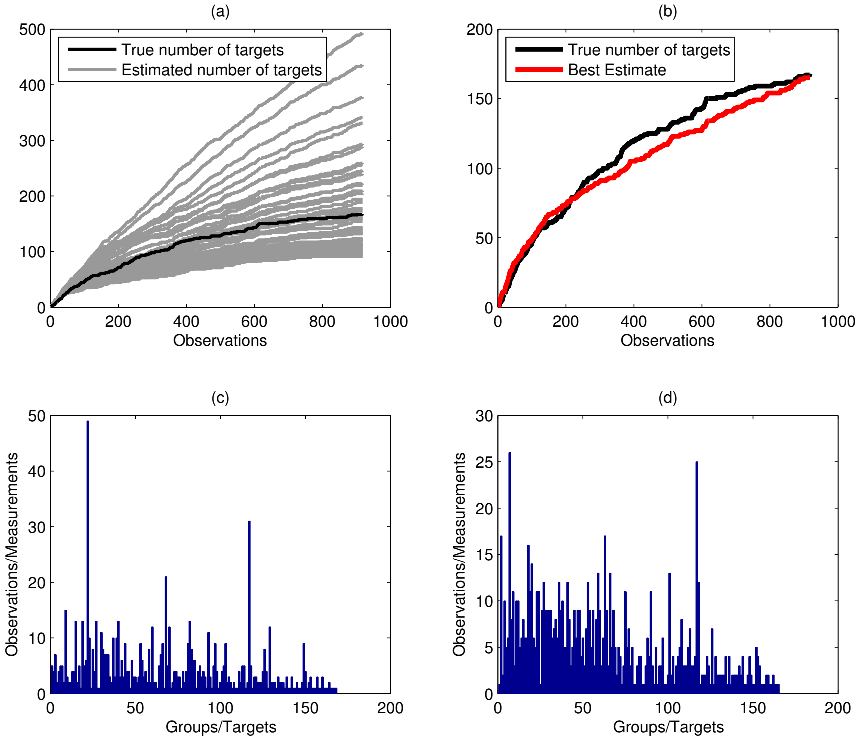

Figure 4.5: (a) Different estimated number of targets in time, (b) Best estimate of the total number of targets, (c) True Group distribution, (d) Group distribution for the best estimate of the total number of targets.

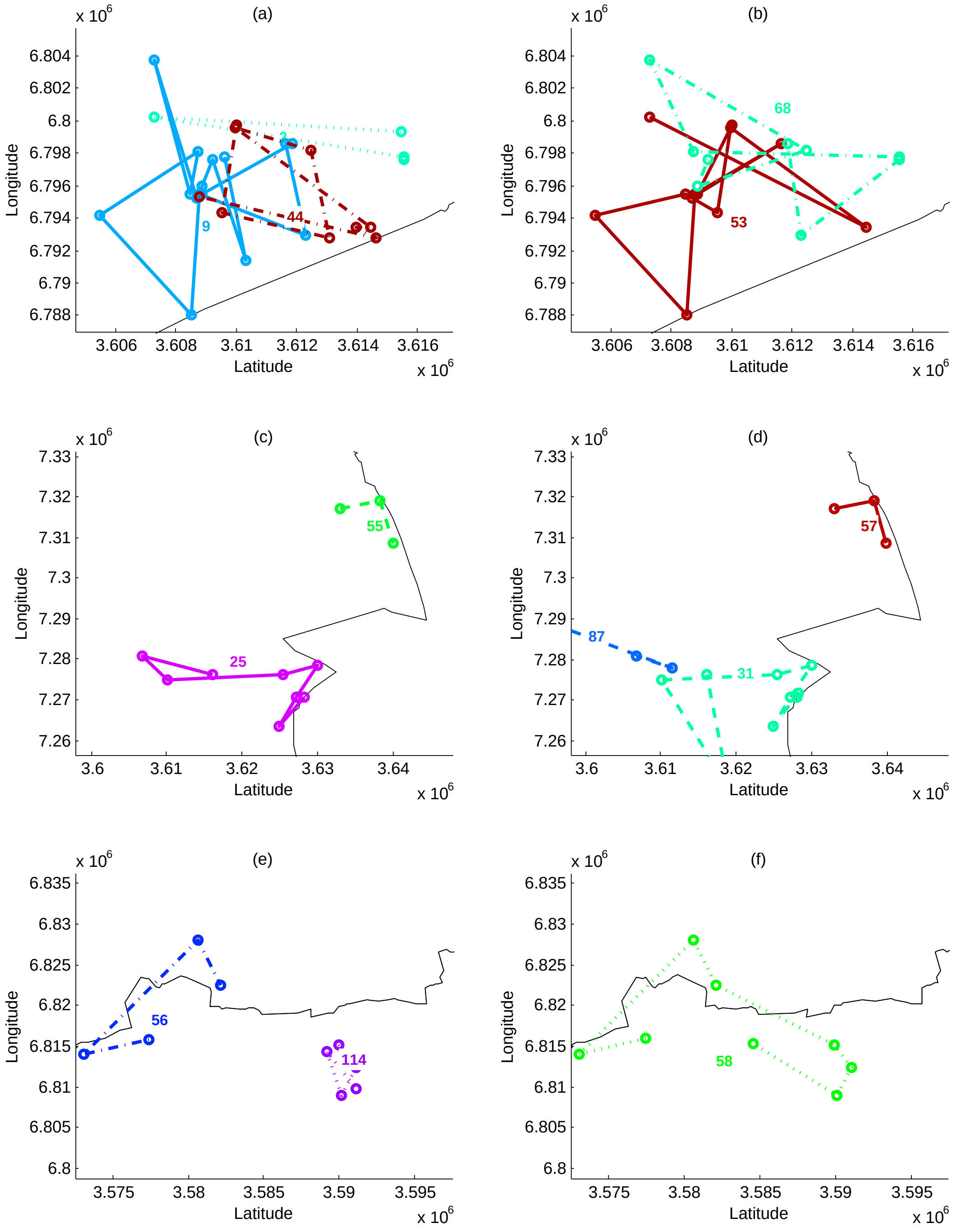

Figure 4.6: Left column: true bear observation groups in three different locations. Right column: corresponding data association results

Dataset 2009

The observation group labels are unassigned in this dataset. Hence, the comparison between the estimated number of targets and the true number of targets in time is impossible. We present the results of the total number of targets for each specie and provide the estimates of the actual animal populations. Both the static model and the random walk model could be applied for the analysis of this dataset and similar estimates for the 'total number of targets' can be generated. Therefore, we demonstrate the results with a single model and present the parameters which generated the best estimates of the animal populations.

We use the random walk model with mainly the same settings as used for the results in the previous section. However, the parameters that were changed for this analysis are presented again for bear, wolf, lynx and wolverine observations. The statistics of the dataset are shown in Tables 3.2 to 3.5. The Figure 4.8(a) shows the bear observations, Figure 4.8(b) shows the wolf observations, Figure 4.8(c) shows the lynx observations and Figure 4.8(d) shows the wolverine observations.

For the bear observations we set $q_x = q_y = 1000^2$ and all the remaining parameters were unchanged. The total number of targets obtained was 139. This value multiplied by a factor of 10 gives the estimate of the bear population in Finland for the year 2009. The group distribution is shown in Figure 4.7.

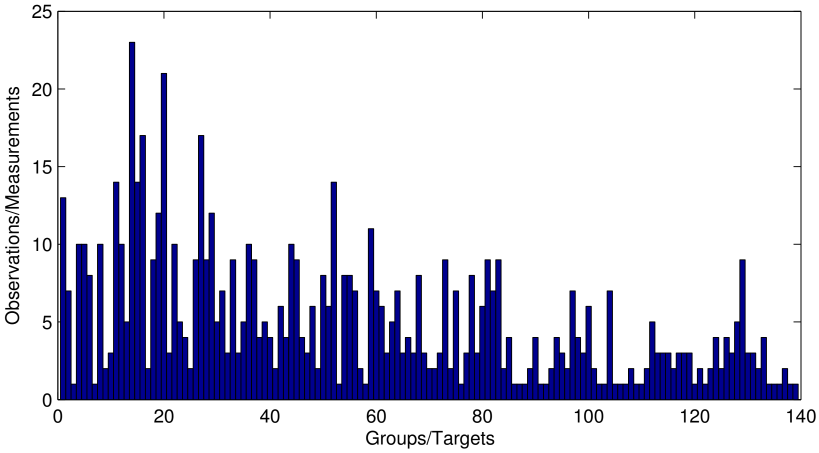

Figure 4.7: Estimated group distribution of bear observations (2009)

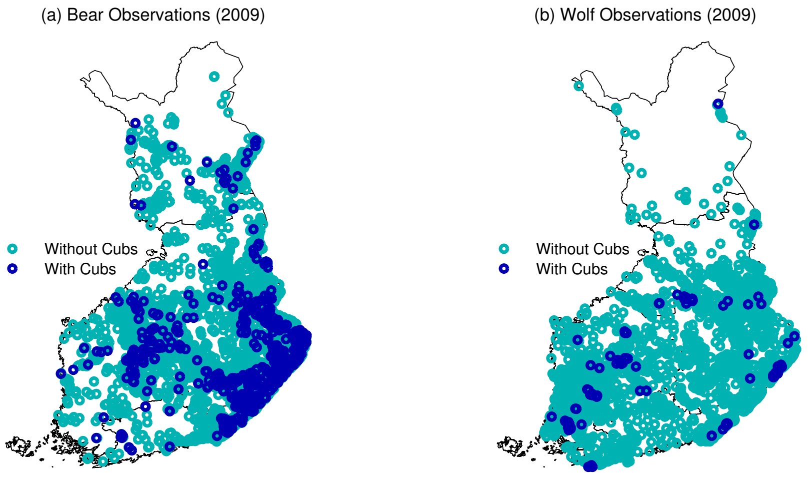
(a) Bear Observations (2009)

(b) Wolf Observations (2009)

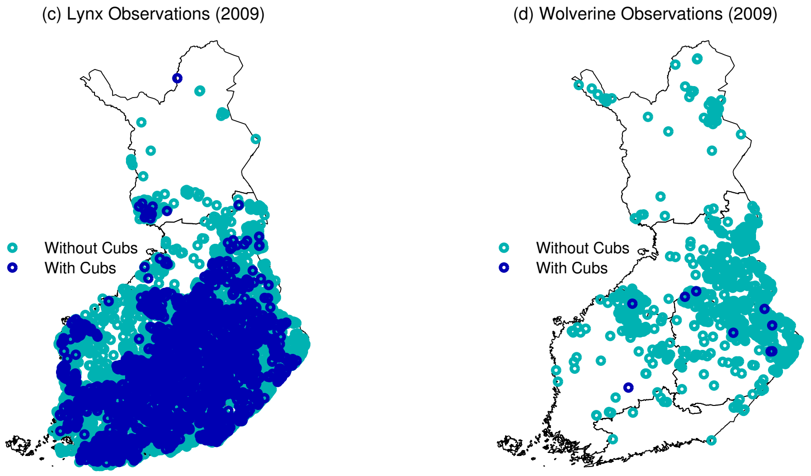
(c) Lynx Observations (2009)

(d) Wolverine Observations (2009)

Figure 4.8: Large carnivore observations in Finland for the year 2009. A single observation can consist of a single individual or a family/pack of animals.

For wolf observations we chose $q_x = q_y = 3000^2$, $\boldsymbol{m}_0 = (0\ 0\ 8\ 8\ 8\ 4\ 4\ 4)^T$ and all the remaining parameters were unchanged. The total number of targets obtained was 15. This value multiplied by a factor of 10 gives the estimate of the wolf population in Finland for the year 2009. The group distribution is shown in Figure 4.9.

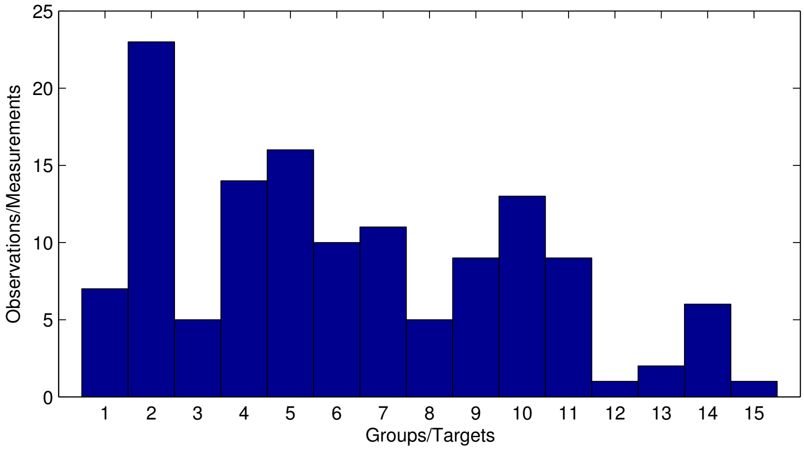

Figure 4.9: Estimated group distribution of wolf observations (2009)

For lynx observations we chose $q_x = q_y = 1000^2$, $\boldsymbol{m}_0 = (0\ 0\ 10\ 10\ 10\ 4\ 4\ 4)^T$ and all the remaining parameters were unchanged. The total number of targets obtained was 402. This value multiplied by a factor of 6 gives the estimate of the lynx population in Finland for the year 2009. The group distribution is shown in Figure 4.10.

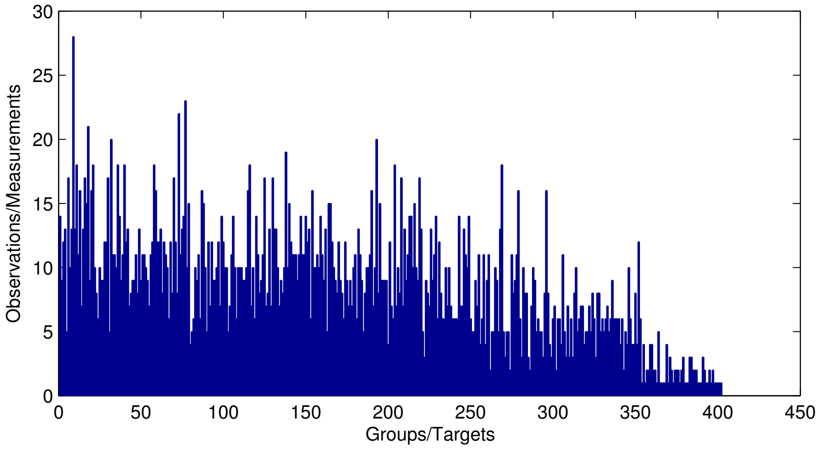

Figure 4.10: Estimated group distribution of lynx observations (2009)

For the wolverine case the number of observations with at least a single adult and a single cub is very low as shown in Table 3.5. Therefore, we use all the observations in the estimation. We chose $q_x = q_y = 1500^2$, $\boldsymbol{m}_0 = (0\ 0\ 11\ 11\ 11\ 4\ 4\ 4)^T$ and all the remaining parameters were unchanged. The total number of targets obtained was 152. In this case, we are unaware of the factor multiplication. Hence, the estimated wolverine population is not projected. The group distribution is shown in Figure 4.11.

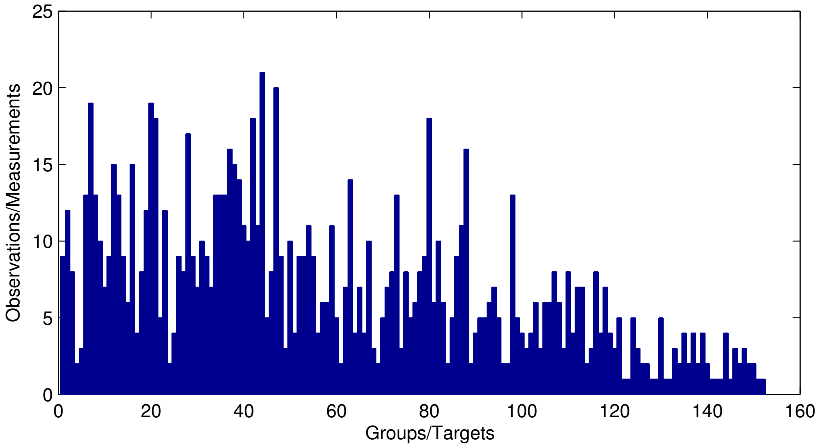

Figure 4.11: Estimated group distribution of wolverine observations (2009)

Chapter 5

Conclusion and Discussion

In this thesis, we have presented a novel approach for the problem of estimating wild animal population from an unconventional dataset. We incorporated animal movement models with the state-space modeling framework for estimating the size of animal populations. We showed the method of formulating the problem as a conditionally linear Gaussian state-space model and recursively estimating the state of the animals. We applied the multiple target tracking methodology for tracking an 'unknown number of targets' to the animal observation datasets.

We developed a computational method to solve the problem of estimating large carnivores in Finland and showed that both static and dynamic models with appropriate parameters generate population estimates that are very close to the ones generated with the manual analysis on the datasets by the Finnish Game and Fisheries Research Institute. The estimation with the static model in particular can be considered close to the standard animal abundance estimation methodology in the sense that we assume the animals to be stagnant. On the other hand, the estimation with the random walk model can be considered more realistic because the animals move during the time between the observations. However, accurate parameterization of this model is difficult due to the large area and time frame of the observations.

The models used in this work were mainly parameterized by intuition and such that the results remain similar to the ones produced by the Finnish Game and Fisheries Research Institute. However, the parameterization of the models needs to be automated. More specifically, a statistical parameter estimation method could be utilized before the application of the Rao-Blackwellized Monte Carlo data association algorithm to the animal datasets. The parameters could be estimated by utilizing individual animal movement datasets, for example, GPS data could be used. Although, RBMCDA comprises both births and deaths of targets, the assumption of an open population including immigration and emigration could also be modeled using the population dynamics models. The models used in this work could be enhanced by incorporating parameters of the habitual and social behavior of the animals. Furthermore, landscape information about the habitats of the animals could also be utilized.

The group labels that were considered to be true for the results in this thesis are not exactly correct. Therefore, further improvement in the original manual analysis is also required. The data based only on sighting information is very unreliable, hence the method of data collection requires improvement. The foot size width was the only attribute measurement useful for the data association process in the RBMCDA, adding more attributes to the state could enhance the accuracy of the associations. We classified the animals into adult and cubs based on foot size and seasonal information. This could be improved by including only a single individual in each observation and providing the exact age of the individual in addition to the foot size.

Another on going phase in this project is the development of a software tool that will aid scientists and researchers in computing the size of wild animal populations automatically. This thesis provides a basis for many new research directions. This work can be extended for other species datasets as well. The computational method provides wildlife managers and researchers with a method of efficiently computing the estimate of an animal population when there are multiple sources of information in the animal datasets and the number of observations are greater than the actual number of animals.

Bibliography

Anderson, D. (2001). The need to get the basics right in wildlife field studies. *Wildlife Society Bulletin*, 29(4):1294–1297.

Anderson-Sprecher, R. and Ledolter, J. (1991). State-space analysis of wildlife telemetry data. *Journal of the American Statistical Association*, 86(415):596–602.

Bar-Shalom, Y. (1987). *Tracking and data association.* Academic Press Professional, Inc.

Bar-Shalom, Y. and Li, X. (1995). Multitarget-multisensor tracking: principles and techniques. *Storrs, CT: University of Connecticut, 1995.*

Bar-Shalom, Y., Li, X., Li, X., and Kirubarajan, T. (2001). *Estimation with applications to tracking and navigation.* Wiley-Interscience.

Blackman, S. and Popoli, R. (1999). *Design and analysis of modern tracking systems.* Artech House Norwood, MA.

Börger, L., Dalziel, B., and Fryxell, J. (2008). Are there general mechanisms of animal home range behaviour? a review and prospects for future research. *Ecology letters*, 11(6):637–650.

Breitenmoser, U. (2000). *Action plan for the conservation of the Eurasian lynx in Europe (Lynx lynx).* Number 18-112. Council of Europe.

Brillinger, D., Preisler, H., Ager, A., Kie, J., and Stewart, B. (2002). Employing stochastic differential equations to model wildlife motion. *Bulletin of the Brazilian Mathematical Society*, 33(3):385–408.

Buckland, S., Anderson, D., Burnham, K., Laake, J., Borchers, D., and Thomas, L. (2004a). *Advanced distance sampling: estimating abundance of biological populations.* Oxford University Press Oxford, UK.

Buckland, S., Goudie, I., and Borchers, D. (2000). Wildlife population assessment: past developments and future directions. *Biometrics*, 56(1):1–12.

Buckland, S., Newman, K., Fernández, C., Thomas, L., and Harwood, J. (2007). Embedding population dynamics models in inference. *Statistical Science*, pages 44–58.

Buckland, S., Newman, K., Thomas, L., and Koesters, N. (2004b). State-space models for the dynamics of wild animal populations. *Ecological modelling*, 171(1-2):157–175.

Delahay, R. and Wilson, G. (2001). A review of methods to estimate the abundance of terrestrial carnivores using field signs and observation. *Wildlife Research*, 28(2):151–164.

Doucet, A., De Freitas, N., and Gordon, N. (2001). *Sequential Monte Carlo methods in practice.* Springer Verlag.

Durban, J. and Elston, D. (2005). Mark-recapture with occasion and individual effects: abundance estimation through bayesian model selection in a fixed dimensional parameter space. *Journal of agricultural, biological, and environmental statistics*, 10(3):291–305.

Gimenez, O., Bonner, S., King, R., Parker, R., Brooks, S., Jamieson, L., Grosbois, V., Morgan, B., and Thomas, L. (2009). Winbugs for population ecologists: Bayesian modeling using markov chain monte carlo methods. *Modeling demographic processes in marked populations*, pages 883–915.

Grewal, M., Andrews, A., and Corporation, E. (2001). *Kalman filtering: theory and practice using MATLAB.* Wiley Online Library.

Julier, S. and Uhlmann, J. (2004). Unscented filtering and nonlinear estimation. *Proceedings of the IEEE*, 92(3):401–422.

Katajisto, J. (2006). *Habitat use and population dynamics of brown bears (Ursus arctos) in Scandinavia.* Doctoral dissertation, University of Helsinki.

Kirubarajan, T. and Bar-Shalom, Y. (2005). Probabilistic data association techniques for target tracking in clutter. *Proceedings of the IEEE*, 92(3):536–557.

Landa, A., Lindén, M., and Kojola, I. (2000). *Action plan for the conservation of wolverines (Gulo gulo) in Europe.* Council of Europe Press, Strasbourg.

Leslie, P. (1945). On the use of matrices in certain population mathematics. *Biometrika*, 33(3):183–212.

Liukkonen, T., Mykrä, S., Bisi, J., and Kurki, S. (2009). Conflicts and compromises in lynx (lynx lynx) conservation and management in finland. *Wildlife Biology*, 15(2):165–174.

Madon, B., Gimenez, O., McArdle, B., Scott Baker, C., and Garrigue, C. (2011). A new method for estimating animal abundance with two sources of data in capture-recapture studies. *Methods in Ecology and Evolution*.

Mills, L., Citta, J., Lair, K., Schwartz, M., and Tallmon, D. (2000). Estimating animal abundance using noninvasive dna sampling: promise and pitfalls. *Ecological Applications*, 10(1):283–294.

Morales, J., Moorcroft, P., Matthiopoulos, J., Frair, J., Kie, J., Powell, R., Merrill, E., and Haydon, D. (2010). Building the bridge between animal movement and population dynamics. *Philosophical Transactions of the Royal Society B: Biological Sciences*, 365(1550):2289.

Newman, K. (1998). State-space modeling of animal movement and mortality with application to salmon. *Biometrics*, pages 1290–1314.

Newman, K., Fernández, C., Thomas, L., and Buckland, S. (2009). Monte carlo inference for state–space models of wild animal populations. *Biometrics*, 65(2):572–583.

Nielsen, A., Bigelow, K., Musyl, M., and Sibert, J. (2006). Improving light-based geolocation by including sea surface temperature. *Fisheries Oceanography*, 15(4):314–325.

Øksendal, B. (2003). *Stochastic differential equations: an introduction with applications*. Springer Verlag.

Patterson, T., Thomas, L., Wilcox, C., Ovaskainen, O., and Matthiopoulos, J. (2008). State-space models of individual animal movement. *Trends in ecology & evolution*, 23(2):87–94.

Pollock, K. (2000). Capture-recapture models. *Journal of the American Statistical Association*, 95(449):293–296.

Pollock, K., Nichols, J., Simons, T., Farnsworth, G., Bailey, L., and Sauer, J. (2002). Large scale wildlife monitoring studies: statistical methods for design and analysis. *Environmetrics*, 13(2):105–119.

Preisler, H., Ager, A., Johnson, B., and Kie, J. (2004). Modeling animal movements using stochastic differential equations. *Environmetrics*, 15(7):643–657.

Ristic, B., Arulampalam, S., and Gordon, N. (2004). *Beyond the Kalman filter: Particle filters for tracking applications.* Artech House Publishers.

Royer, F., Fromentin, J., and Gaspar, P. (2005). A state-space model to derive bluefin tuna movement and habitat from archival tags. *Oikos*, 109(3):473–484.

Salvatori, V. and Linnell, J. (2005). Report on the conservation status and threats for wolf (canis lupus) in europe. *Councel of Europe. PVS/Inf (2005)*, 16.

Särkkä, S. (2006). *Recursive Bayesian inference on stochastic differential equations.* Doctoral dissertation, Helsinki University of Technology.

Särkkä, S., Vehtari, A., and Lampinen, J. (2007). Rao-Blackwellized particle filter for multiple target tracking. *Information Fusion*, 8(1):2–15.

Schwarz, C. and Seber, G. (1999). Estimating animal abundance: review iii. *Statistical Science*, pages 427–456.

Seber, G. (1986). A review of estimating animal abundance. *Biometrics*, pages 267–292.

Smouse, P., Focardi, S., Moorcroft, P., Kie, J., Forester, J., and Morales, J. (2010). Stochastic modelling of animal movement. *Philosophical Transactions of the Royal Society B: Biological Sciences*, 365(1550):2201.

Southwood, R. and Henderson, P. (2000). *Ecological methods.* Wiley-Blackwell.

Thompson, W., White, G., and Gowan, C. (1998). *Monitoring vertebrate populations.* Academic Press San Diego, California, USA.

White, G. (2000). Modeling population dynamics. *Ecology and management of mammals in North America. Prentice-Hall, Upper Saddle River, New Jersey*, pages 84–107.

Wikman, M. (2010). *Monitoring game abundance in Finland in 2010. Riista- ja kalatalous - Selvityksiä.* Finnish Game and Fisheries Research Institute.

Witmer, G. (2005). Wildlife population monitoring: some practical considerations. *Wildlife Research*, 32(3):259–263.